

# **Design and simulation of Single-stage bidirectional inverter suitable for photovoltaic application**

*A Thesis Submitted in Partial Fulfilment of the Requirements for  
the  
Degree of Master of Electrical Engineering*

*By*

**SAPRATIV SAHA**

Examination Roll No.: **M4ELE19002**

Registration No. : **140654 of 2017-18**

**JADVPUR UNIVERSITY**

*Under the guidance of*

**Dr. DEBASHIS CHATTERJEE**

**Electrical Engineering Department**

**Faculty of Engineering and Technology**

**JADAVPUR UNIVERSITY**

**KOLKATA- 700032, W.B. INDIA**

**JADAVPUR UNIVERSITY**

**FACULTY OF ENGINEERING AND TECHNOLOGY**

**ELECTRICAL ENGINEERING DEPARTMENT**

**KOLKATA- 700032, INDIA**

## **CERTIFICATE OF RECOMMENDATION**

I hereby recommended that the thesis titled “**Design and simulation of Single-stage bidirectional inverter suitable for photovoltaic application**”, submitted by **SAPRATIV SAHA** (Registration No. 140654 of 2017-18), in partial fulfilment of the requirement for the degree of “Master of Electrical Engineering” of Jadavpur University has been carried out by him under our guidance and supervision. The project, in our opinion, is worthy of its acceptance.

### **SUPERVISOR**

---

**Prof. Debashis Chatterjee**

Professor  
Electrical Engineering Department,  
Jadavpur University

### **COUNTERSIGNED**

---

***Prof. Kesab Bhattacharyya***

Head, Dept. of Electrical Engineering,  
Faculty of Engineering and Technology,  
Jadavpur University

---

***Prof. Chiranjib Bhattacharjee***

Dean,  
Faculty of Engineering and Technology,  
Jadavpur University

**JADAVPUR UNIVERSITY**

**KOLKATA- 700032, INDIA**

**FACULTY OF ENGINEERING AND TECHNOLOGY**

**ELECTRICAL ENGINEERING DEPARTMENT**

**CERTIFICATE OF APPROVAL\***

*The foregoing thesis is hereby approved as a creditable study of Master of Electrical Engineering and presented in a manner satisfactory to warrant its acceptance as a prerequisite to the degree for which it has been submitted. It is understood that by this approval the undersigned do not necessarily endorse or approve any statement made, opinion expressed or conclusion therein but approve this thesis only for the purpose for which it is submitted.*

**Final Examination for Evaluation of the Thesis**

1. \_\_\_\_\_

2. \_\_\_\_\_

(Signature of Examiners)

\*Only in case the thesis is approved

# **DECLARATION OF ORIGINALITY AND COMPLIANCE OF ACADEMIC ETHICS**

---

I hereby declare that the thesis entitled “**Design and simulation of Single-stage bidirectional inverter suitable for photovoltaic application**” contains literature survey and original research work as part of the course of Master of Engineering studies. All the information in this document has been obtained and presented in accordance with academic rules and ethical conduct.

I also declare that, as required by these rules and conduct, I have fully cited and referenced all material and results that are not original to this work.

Name : SAPRATIV SAHA

Exam Roll no. : M4ELE19002

Registration no. : 140654 of 2017-18

Thesis Name : DESIGN AND SIMULATION OF SINGLE-STAGE  
BIDIRECTIONAL INVERTER SUITABLE FOR PHOTOVOLTAIC  
APPLICATION

Signature with date :

---

## ACKNOWLEDGEMENT

---

With a great pleaser, I express my deep sense of gratitude to my supervisors, **Prof. Debashis Chatterjee**, Department of Electrical Engineering of Jadavpur University for giving me the invaluable opportunity to work in this exciting field. I am obliged and grateful to him for guidance, suggestions and encouragement throughout the project. I will always remain thankful to him for his patience with me. As a beginner in this field, I learn how to do research work from him.

I would also wish to express my sincere gratitude to **Professor Subrata Paul, Professor Amitava Chatterjee, Associate Professor Nikhil Mondal, Assistant Professor Susanta Roy, Professor Suparna Kar Chaudhury, Professor Madhab Roy, Professor Sugata Munshi** and **Professor Palash Kr. Kundu** Department of Electrical Engineering, Jadavpur University, for their encouragement, advice and motivation during the coursework.

I am also thankful to **Dr. Kesab Bhattacharyya**, Head, Department of Electrical Engineering, Jadavpur University, for providing the necessary facilities for carrying out this thesis work.

I am also thankful to rest of the research scholars **Mr. Soumyajit Ghosh, Mrs. Swati Suman, Mr. Sarang Khadtare** of Drives laboratory for their support throughout the tenure of the thesis work.

I would like to thank my dear friend **Mr. Toulik Chakraborty, Mr. Meghnad Hembram, Mr. Pranab Sur, Mr. Souvik Saha, Mr. Banibrata Ghosh, Mrs. Payel Banerjee, Mrs. Medha Nag, Mr. Deepesh Das, Mr. Sandip Bera, Mr. Ritam Chakrabarty**, PG scholar, E.E. Department, from whom I received immense support. I would like to convey my soulful thankfulness to the rest of the PG scholars of E.E. Department for their moral support during this course work. I am extremely grateful to my parents for their constant support and motivation, without that I would not have come to this stage. This thesis, a fruit of the combined efforts of my family members, is dedicated to them as a token of love and gratitude.

Above all, it is the wish of the almighty that I have been able to complete this work.

Thank you,

**Saprativ Saha**

---

*DEDICATED TO MY  
PARENTS*

## **Table of contents:**

---

Certificate of Recommendation	ii
Certificate of Approval	iii
Declaration of Originality and Complains of Academic Ethics	iv
Acknowledgements	v
Table of Contents	vii
List of Figures	ix

---

<b>CHAPTER</b>	<b>PAGE</b>
<b>Chapter-1.</b> <b>A.C. Power supplies</b> .....	<b>1</b>
<b>Chapter-2.</b> <b>Single stage inverters</b> .....	<b>3</b>
a) Z-Source inverter.	
b) dc/dc converter derived inverters.	
• Study on dc/dc converter derived inverters.	
○ Differential connection of load.	
➤ Buck inverter.	
▪ Matlab simulation study of Buck inverter.	
➤ Boost inverter.	
▪ Matlab simulation study of Boost inverter.	
➤ Buck-Boost inverter.	
➤ Single stage dual Flyback inverter.	
➤ Dual active bridge converter with unfolder bridge.	
▪ Calculation of power flow of DAB converter.	
➤ Flyback converter with unfolder bridge.	
<b>Chapter-3.</b> <b>Circuit operation with current mode control.</b> .....	<b>16</b>
• Discharging.	
• Charging.	
<b>Chapter-4.</b> <b>State-space averaging in CCM.</b> .....	<b>20</b>
• State-space averaging of Buck-Boost converter (at CCM).	
• Transfer function analysis.	
• First order model of current mode controlled Buck-Boost converter.	

- Matlab simulation study of RHP zero effect.

---

**CHAPTER**

**PAGE**

---

<b>Chapter-5.</b>	<b><u>Single-stage inverter operation at DCM.</u></b>	<b>31</b>
	<ul style="list-style-type: none"> <li>• Calculation of <math>L_m</math> for DCM operation.</li> <li>• Matlab simulation study of single-stage inverter at DCM.</li> </ul>	
<b>Chapter-6.</b>	<b><u>Single-stage inverter operation extended to three-phase.</u></b>	<b>36</b>
	<ul style="list-style-type: none"> <li>• Description of three phase unfolder bridge operation with single stage Flyback converter.</li> <li>• Matlab simulation study of single stage three phase system.</li> </ul>	
<b>Chapter-7.</b>	<b><u>Study of three phase scheme of single stage conversion.</u></b>	<b>42</b>
	<ul style="list-style-type: none"> <li>• D-Q control theory.</li> <li>• P-Q control.</li> <li>• Matlab simulation study of three phase scheme.</li> </ul>	
<b>Chapter-8.</b>	<b><u>Discussion and conclusion</u></b>	<b>47</b>
	<b><u>References</u></b>	<b>48</b>



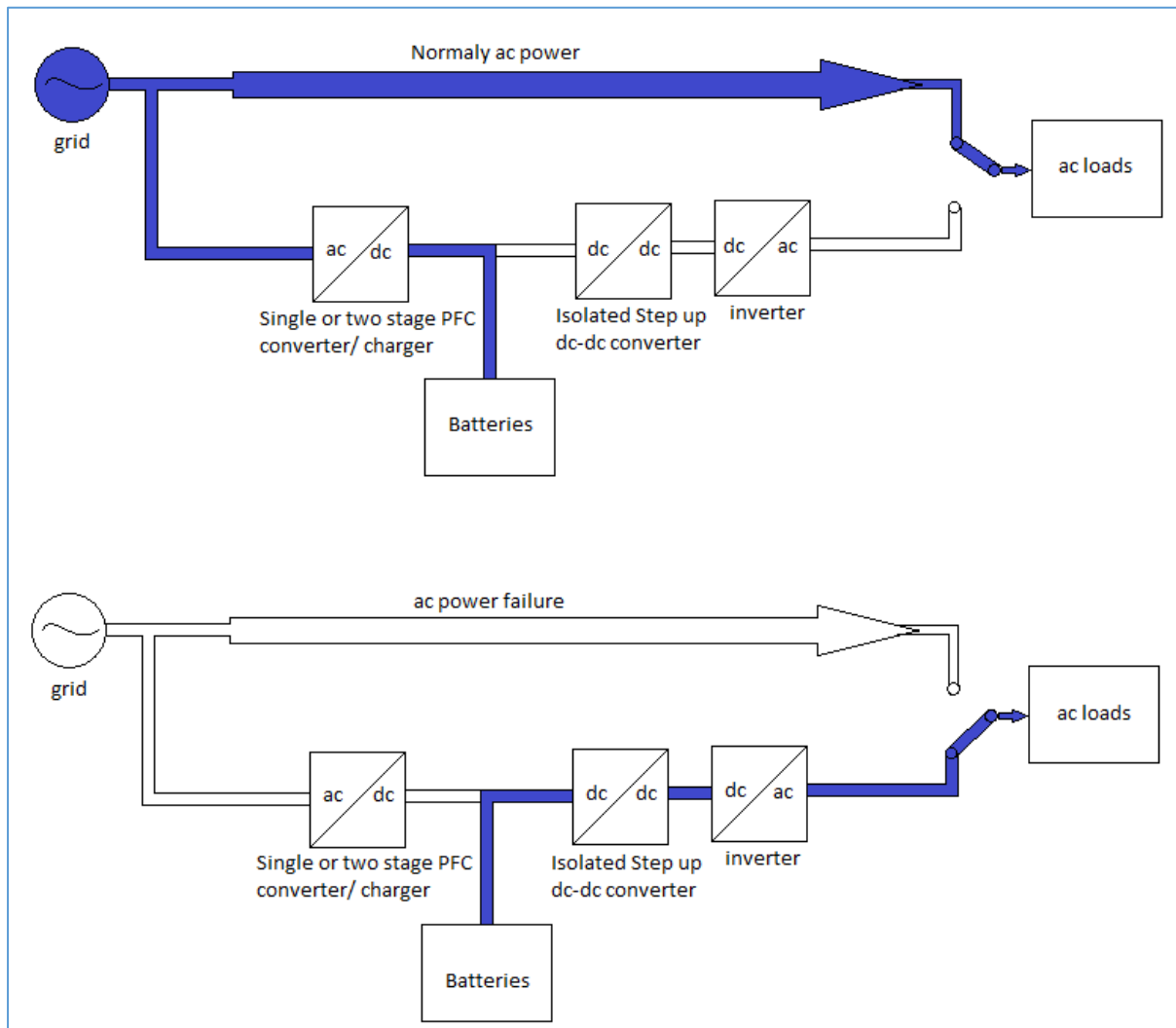
## **List of figures:**

<b>Figure number</b>	<b>Description</b>	<b>Page</b>
1.1	The conventional stand-alone generating system with three or four power conversion stages	1
1.2	Stand-alone generating system with single power conversion stage	2
2.1	Bidirectional Z-source inverter	3
2.2	Matlab model of Buck inverter	5
2.3	Sinusoidal Duty cycle generation	5
2.4	Buck inverter output voltage waveform	6
2.5	Principle of boost inverter	6
2.6	Two directional boost converters	7
2.7	Matlab model of Boost inverter	8
2.8	Boost inverter output voltage and inductor current	8
2.9	Output voltage and current of Boost inverter	9
2.10	Buck-Boost inverter	9
2.11	Single stage dual Flyback inverter	10
2.12	Circuit diagram of Dual active bridge converter	11
2.13	Operating waveforms (a) A-to-B mode and (b) B-to-A mode	11
2.14	Bidirectional DAB inverter for the stand-alone generating system with single power-conversion stage	14
2.15	Circuit Diagram of Flyback converter with unfolded bridge	15
3.1	Magnetizing Inductor Current, Primary Switch current and dc link current respectively at DCM	16
3.2	Gate switching pulse generation block diagram	16
3.3	Hysteresis band current controller for gate pulse generation	17
4.1	Switching sequence diagram	20
4.2	Capacitor voltage drop for duty cycle increment	27
4.3	Immediate Inductor current rise for duty cycle increment	28
4.4	Simulink model of Flyback converter with resistive load	30
4.5	Simulated waveform of inductor current and output voltage of Flyback converter due to incremental step change in duty cycle from $d=0.55$ to $d=0.552$	30
5.1	Inductor current at DCM during half cycle of utility grid line	31
5.2	Grid connected Single-stage inverter (Discharging mode)	32
5.3	Switch current waveform for $f_{sw} = 6 \text{ kHz}$ (At DCM)	33
5.4	Dc bus voltage waveform	33
5.5	Simulated waveform of a) dc link current, b) output voltage(x10) & output current, c) grid current at discharging mode	34
5.6	Single-stage inverter at charging mode with $f_{inv} = 6 \text{ kHz}$ , duty cycle=50%	34

5.7	Simulated waveform of a) dc link current, b) output voltage(x10) & output current, c) grid current at charging mode	35
5.8	Input dc current waveform of Single-stage inverter at charging mode	35
6.1	Three phase Unfolder Bridge with graphical representation of its operation	36
6.2	Pulse Sequence & pulse relation of switches of three phase Unfolder Bridge	37
6.3	Matlab model of three phase Unfolder Bridge	38
6.4	Unfolder bridge operation at window 1	38
6.5	Unfolder bridge operation at window 2	39
6.7	dc link currents( $i_{f1}$ & $i_{f2}$ ) and reconstructed ac currents( $i_a$ , $i_b$ & $i_c$ )	39
6.8	Flyback converter with three phase unfolder with three phase star connected R-L load	40
6.9	a) Output Line voltage, b) 90 degree phase shifted two dc bus voltages ( $f=150$ Hz), c) Output line voltage (three phase), d) Output load current (three phase)	40
6.10	Flyback converter with three phase unfolder (Grid connected, without transformer)	41
6.11	a) Output Line voltage, b) 90 degree phase shifted two dc bus voltages ( $f=150$ Hz), c) Output phase voltage (three phase), d) Output load current (three phase)	41
7.1	Matlab model of three phase scheme	42
7.2	P-Q control block	45
7.3	Output voltage and grid current waveform	46
7.4	P-Q curve	46

# CHAPTER-1

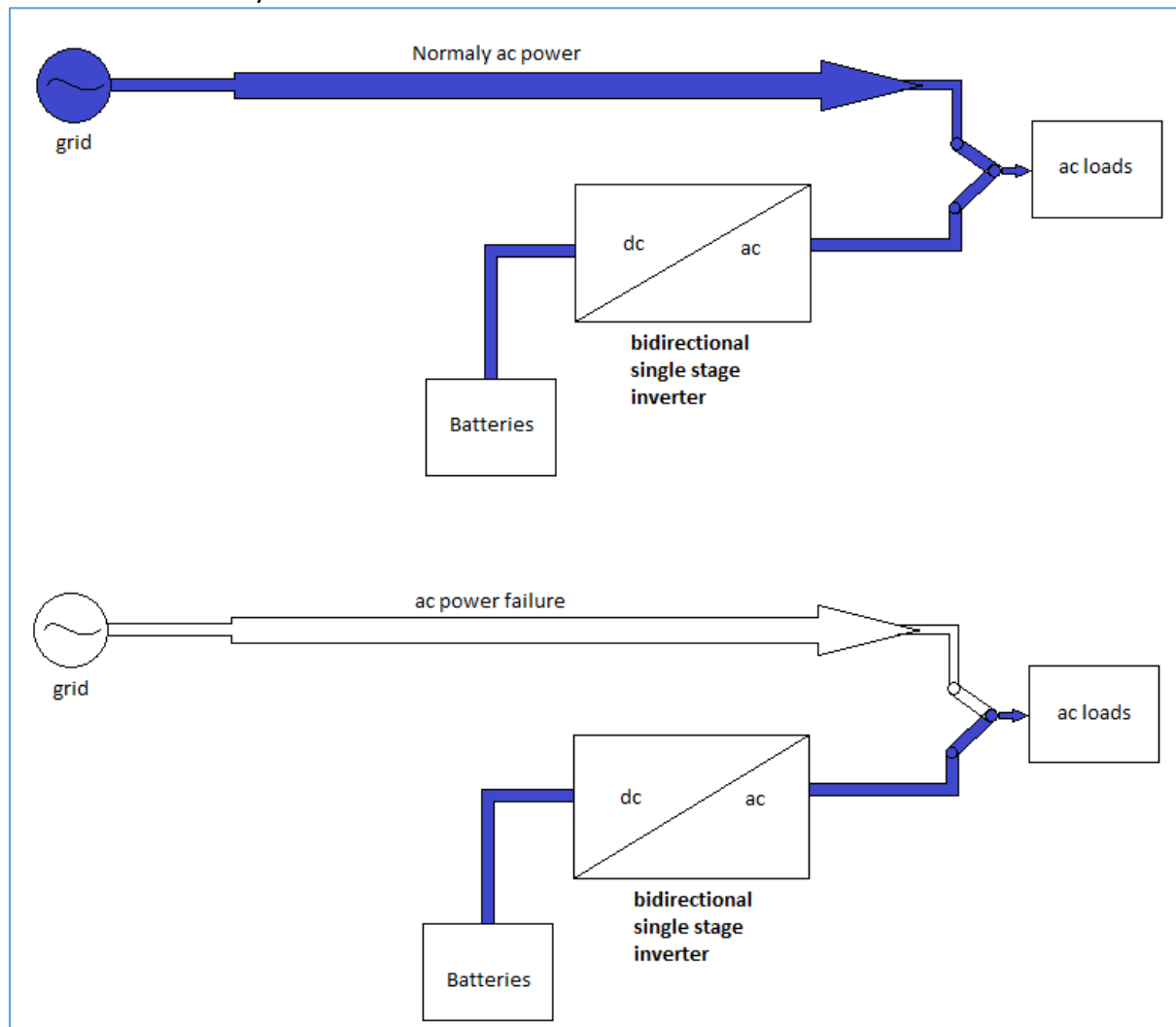
## AC Power Supplies:



**The conventional stand-alone generating system with three or four power conversion stages, Figure 1.1**

Generally stand-alone generating systems require high efficiency, high reliability, small size, and low cost. For household electric supply, the cost and size are important elements. As an uninterruptible power supply (UPS) used in internet data centres, hospitals, and militaries, it is also important to provide reliable and high quality power since a power failure can cause serious problems such as data loss, injuries, fatalities, or business disruption. The off-line UPS is now the most commonly used technology for supplying power to critical loads such as computers and medical equipment. When utility power is not available, it provides regulated emergency power to the connected equipment by supplying power from a separate source. In the off-line UPS system, the load is directly connected to the ac power source, typically the grid, or ac loads. When the grid fails or goes below a minimum level, the off-line UPS blocks the incoming grid power and delivers power to the ac load via a dc-ac inverter system with an internal storage battery. The conventional stand-alone generating system for off-line UPSs has three or four power conversion stages as shown. The three or

four power conversion stages, the hard switching in the inverter, and the use of more reactive elements lead to reduced efficiency, power density, and reliability and increase the cost of the overall system.



**Stand-alone generating system with single power conversion stage, Figure 1.2**

To solve these problems, **single-stage isolated bidirectional inverters** have recently become a major research topic and have been proposed as an interface of the stand-alone power generating system.

## CHAPTER- 2

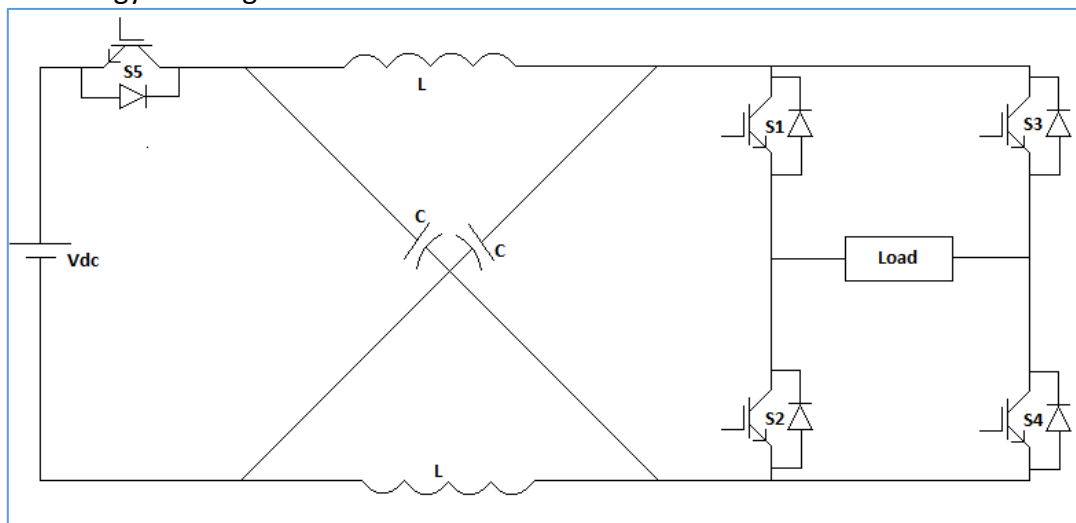
### Single stage inverters (with bidirectional property)

Single-stage inverters can step up and down the dc voltage and be modulated to achieve a sinusoidal output current or voltage.

There are two types of single stage inverters a) Z-source inverter, b) dc-dc converter derived inverters. Dc-dc converter derived inverters can be 1) Buck inverter, 2) Boost inverter, 3) Buck-Boost inverter, 4) Single stage dual Flyback inverter, 5) Dual active bridge converter and Flyback converter with unfolded bridge.

#### a) Z-source inverter

Z-source inverter consists of a unique L-C circuit which handles shoot through states and boosts the output voltage. Thus shoot through cannot destroy the inverter. Z-source inverter has both buck and boost capability with single structure. To make inductor current almost constant and to keep the Z-source inverter in CCM, choice of inductor value should be great enough. In DCM, inverter output voltage becomes uncontrollable and increases infinitely under small inductance. The bidirectional-ZSI is used to avoid this shortcoming and provide energy exchange in both direction between dc and ac side.



**Bidirectional Z-source inverter, Figure 2.1**

The main disadvantage of basic ZSI topology is that line current becomes discontinuous in boost mode operation. So there is a large filter requirement which is not desired. A new topology quasi-ZSI overcomes this disadvantage. Here the voltage of single capacitor is lower than the capacitor voltage of basic ZSI. By common earthing of power input source and D.C. link bus common-mode noise can be reduced. In **bidirectional Z-Source**, switching pulse of **S<sub>5</sub>** must be complementary of shoot-through signal.

## b) dc/dc converter derived inverter

- Study on dc/dc converter derived inverters:

- ❖ Differential connection of the load:

In inverter applications, where either polarity is required, a converter is required which is capable of producing an output voltage of either polarity. By variation of duty cycle in the correct manner, a pure sinusoidal output voltage having no dc bias can be obtained. dc/dc converter derived inverter can be of many types. Some basics of them are discussed here.

- Buck inverter

Suppose there are two buck converters having output voltages of  $V_1$  &  $V_2$ . If the load is connected differentially across the two converters then output voltage,  $V = V_1 - V_2$ .

If converter1 is driven with duty cycle =  $D$ , and converter2 is driven with duty cycle =  $(1 - D) = D'$ , and input voltage is equals to  $V_{in}$ .

Then,  $V_1 = D V_{in}$ , and  $V_2 = D' V_{in}$ .

Hence,  $V = V_1 - V_2$

$$= D V_{in} - D' V_{in}$$

$$= (2D - 1)V_{in}$$

At,  $D = 0.5$ ,  $V = 0$ . If  $D > 0.5$ ,  $V > 0$  and for  $D < 0.5$ ,  $V < 0$ .

So, by varying the duty cycle sinusoidally around the quiescent point 0.5, we can get sinusoidal output voltage. This type of control is done by sliding mode controller. But for understanding of the concept by checking through MATLAB,

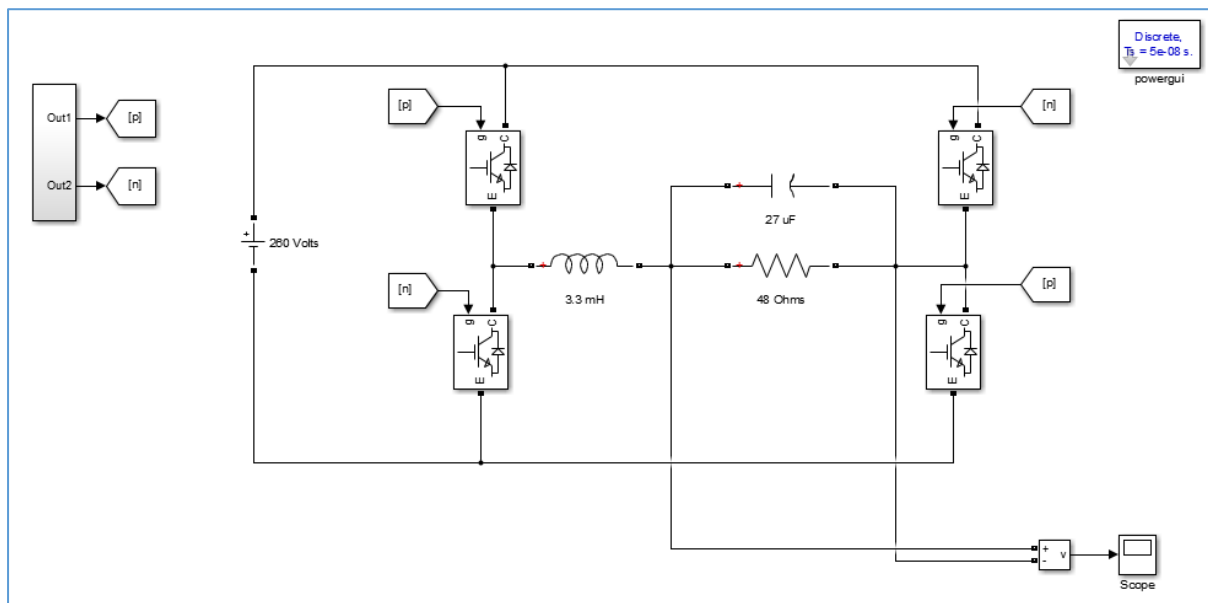
Let,  $D = 0.5 + m_d \sin\omega t$ ; ( $0 < m_d < 0.5$ )

Hence,  $V = [2 * (0.5 + m_d \sin\omega t) - 1] V_{in}$

$$= 2m_d V_{in} \sin\omega t, \quad \text{A pure sinusoid.}$$

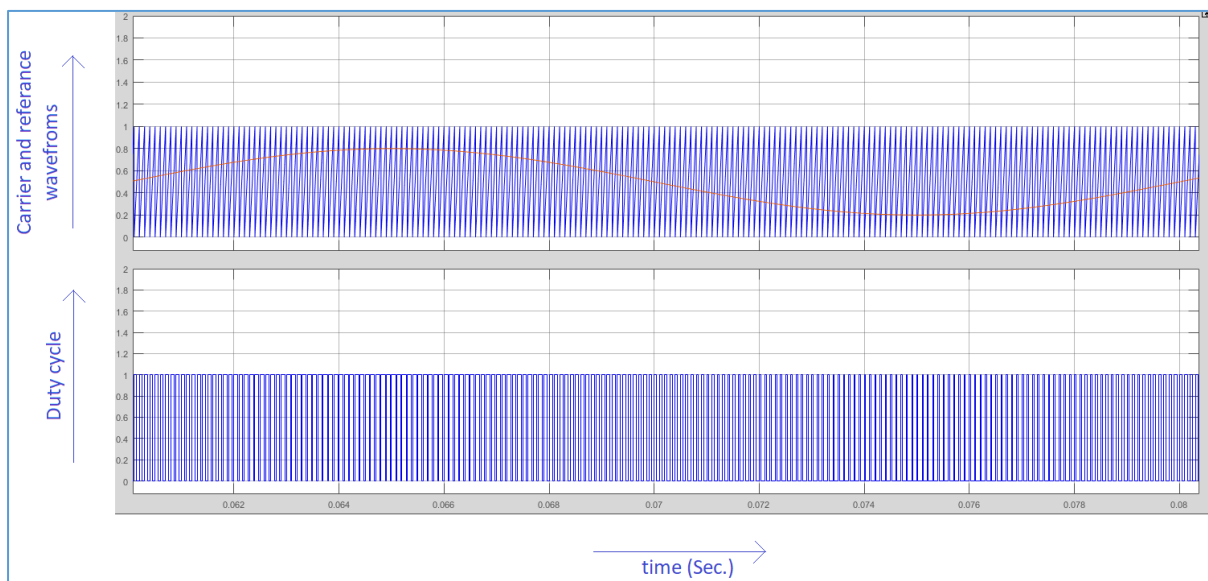
By comparing a carrier sawtooth waveform of unit amplitude with a reference  $(0.5 + m_d \sin\omega t)$ , we can get sinusoidally varying duty cycle around  $D=0.5$  and get sinusoidal output voltage.

✓ Matlab simulation study of Buck inverter:

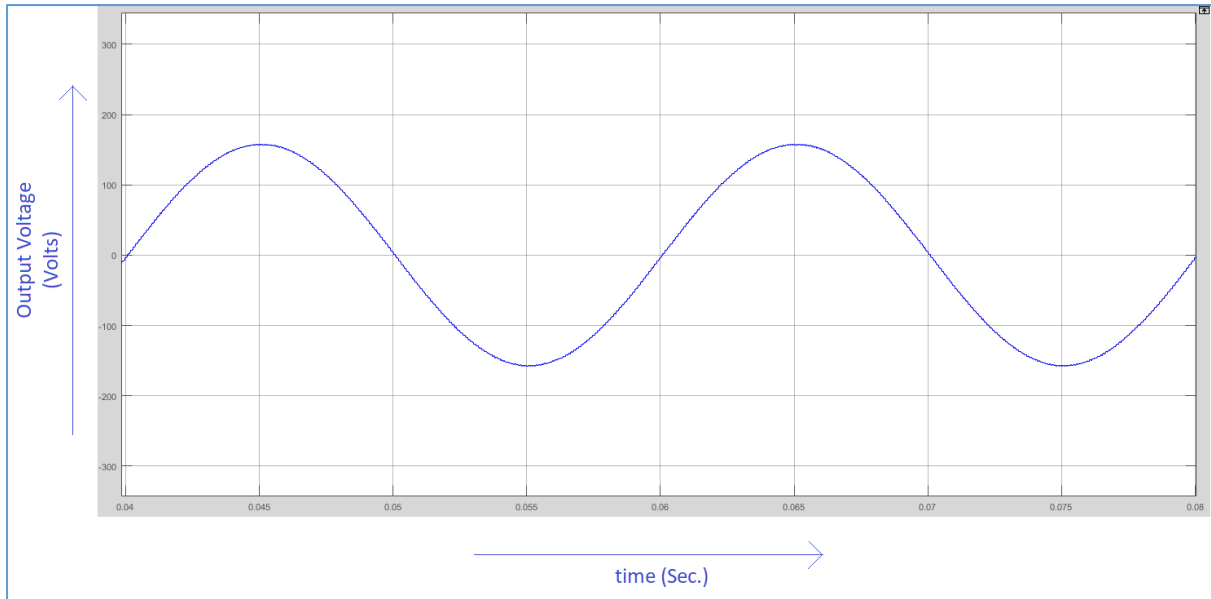


**Matlab model of Buck inverter, Figure 2.2**

With a reference  $(0.5 + 0.3 \sin(2 * \pi * 50 * t))$ , and sawtooth carrier wave of 10 kHz, unit amplitude, we can get the sinusoidally varying duty cycle around  $D=0.5$ .



**Sinusoidal Duty cycle generation, Figure 2.3**



**Buck inverter output voltage waveform, Figure 2.4**

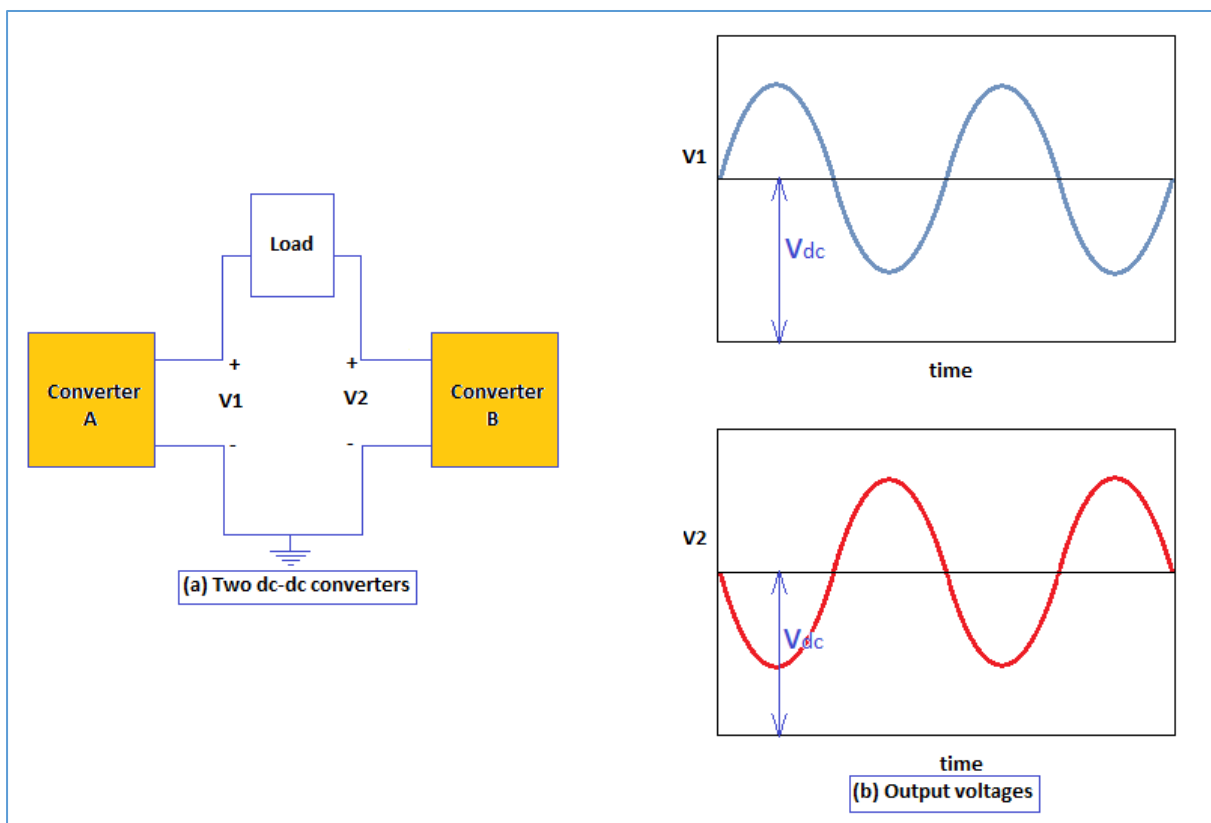
### ➤ Boost inverter

Two dc-dc converters feeding a load. The two dc converter produce a dc-biased sine wave output such that each source produces only a unipolar voltage. The modulation of each converter is  $180^\circ$  out of phase with the other so that the voltage excursion across the load is, maximized. Thus, the output voltages of the converters are described by

$$V_1 = V_{dc} + V_m \sin\omega t \text{ and } V_2 = V_{dc} - V_m \sin\omega t$$

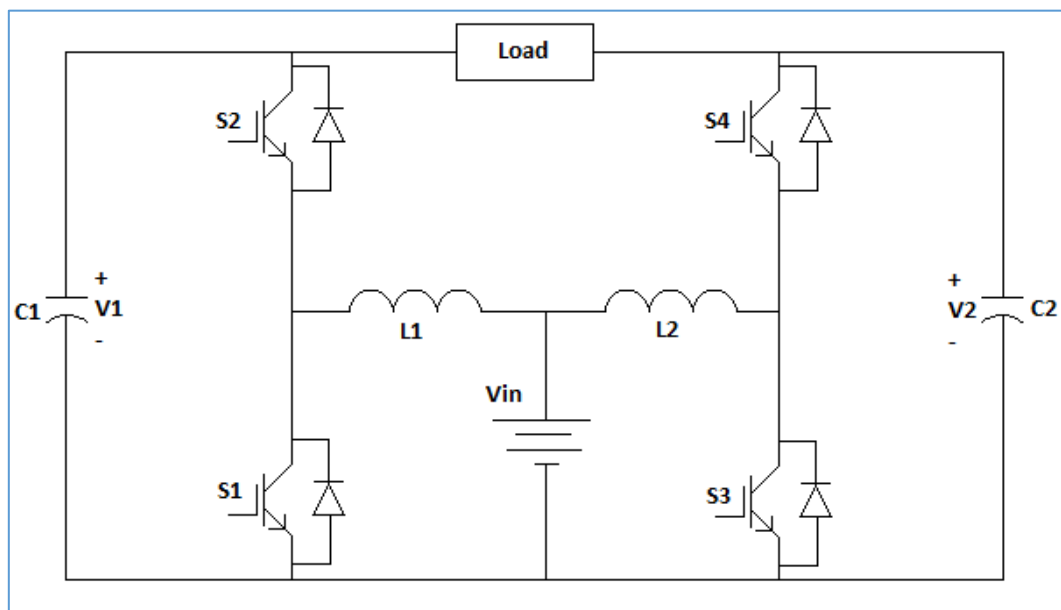
Thus the output voltage is sinusoidal as given by

$$V = V_1 - V_2 = 2V_m \sin\omega t$$



**Principle of boost inverter, Figure 2.5**





**Two directional boost converters, Figure 2.6**

The output of inverter can be controlled by one of the two methods

(1) Use a duty cycle ' $D$ ' for 'converter A' and a duty cycle ' $(1 - D)$ ' for 'converter B'.

(2) Use a different duty cycle for each converter such that each converter produces a dc-biased sine wave output.

The second method is preferred and it uses controller for both converters which makes the capacitor voltages  $V_1$  and  $V_2$  follow dc biased sinusoidal reference voltage.

Hence, the output voltage of boost inverter is

$$\begin{aligned}
 V &= V_1 - V_2 \\
 &= \frac{1}{1-D} - \frac{1}{D} \\
 &= \frac{(2D - 1)}{D(1 - D)}
 \end{aligned}$$

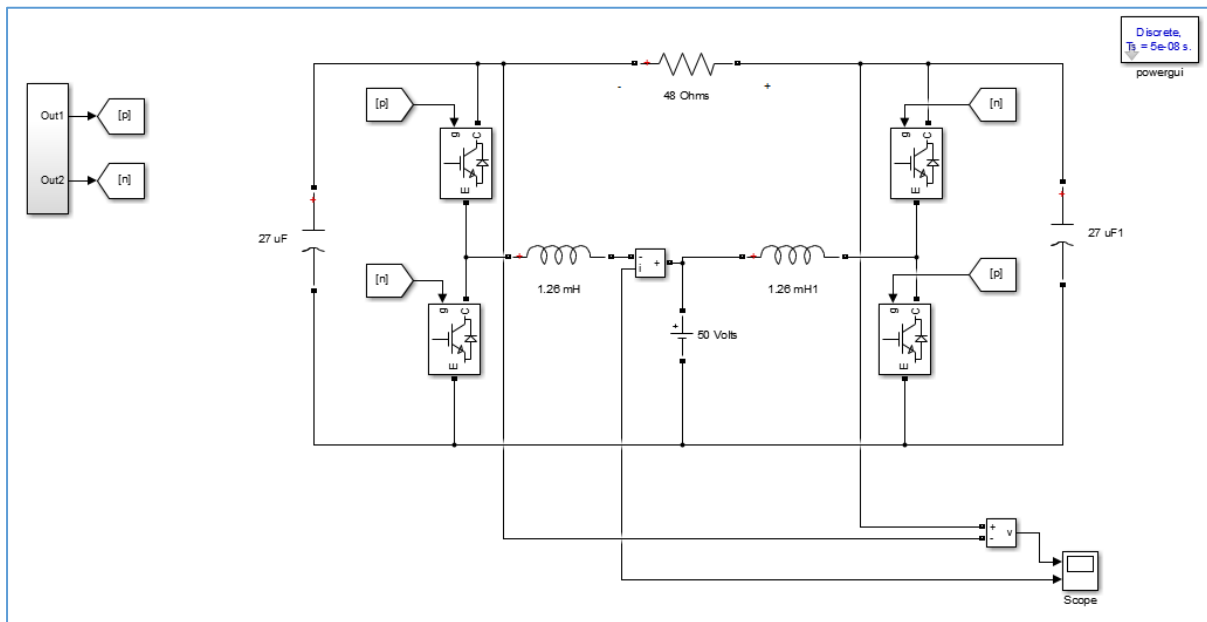
At,  $D = 0.5$ ,  $V = 0$ . If  $D > 0.5$ ,  $V > 0$  and for  $D < 0.5$ ,  $V < 0$ .

So, by varying the duty cycle sinusoidally around the quiescent point  $D=0.5$ , we can get sinusoidal output voltage. But here the output voltage will be sinusoidal between a small range around quiescent point  $D = 0.5$  as boost converter gain is a non-linear function of  $D$ . So, it is better to use controller for both converters which makes the capacitor voltages  $V_1$  and  $V_2$  follow dc biased sinusoidal reference voltage.

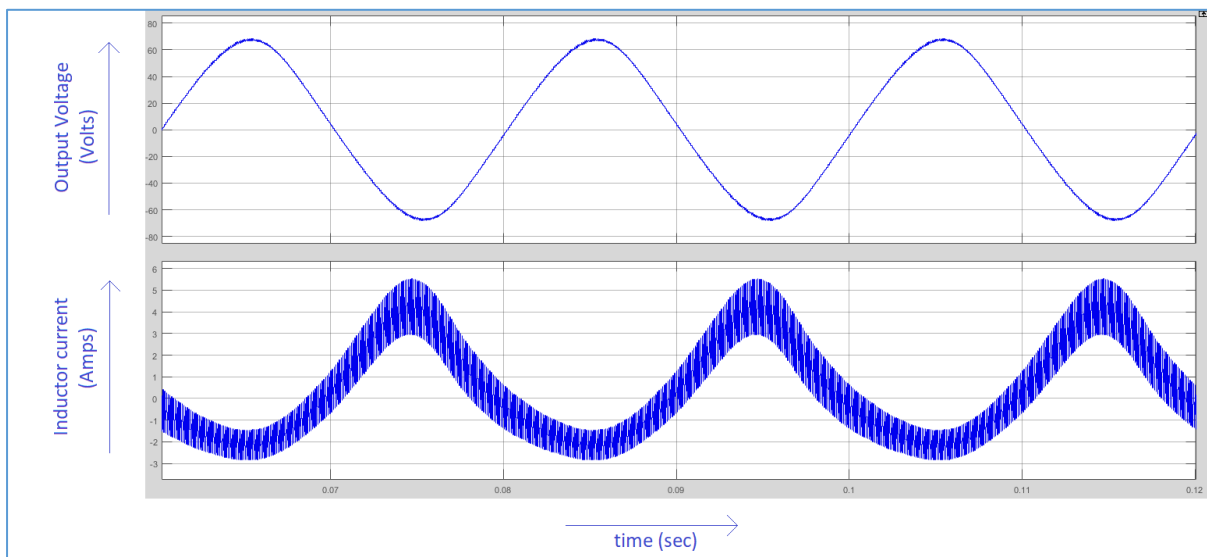
Boost inverter can give output voltage either greater than or less than input voltage depending upon the duty cycle.

✓ Matlab simulation study of Boost inverter:

Similar to buck inverter, here also have used  $D = 0.5 + m_d \sin\omega t$  for observation.  $m_d = 0.15$ .



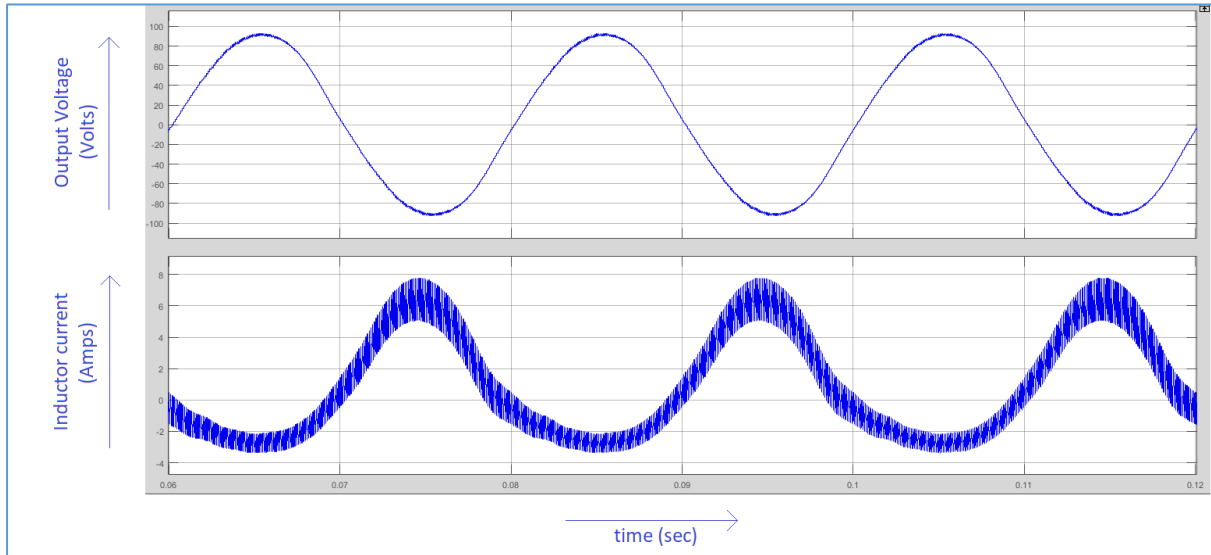
**Matlab model of Boost inverter, Figure 2.7**



**Boost inverter output voltage and inductor current, Figure 2.8**

For higher output voltage, due to nonlinear curve of gain vs duty cycle, output voltage will not follow sinusoidal. So there will be some harmonics at output voltage. To minimize that effect, have injected third harmonic in duty ratio modulation by using following reference,

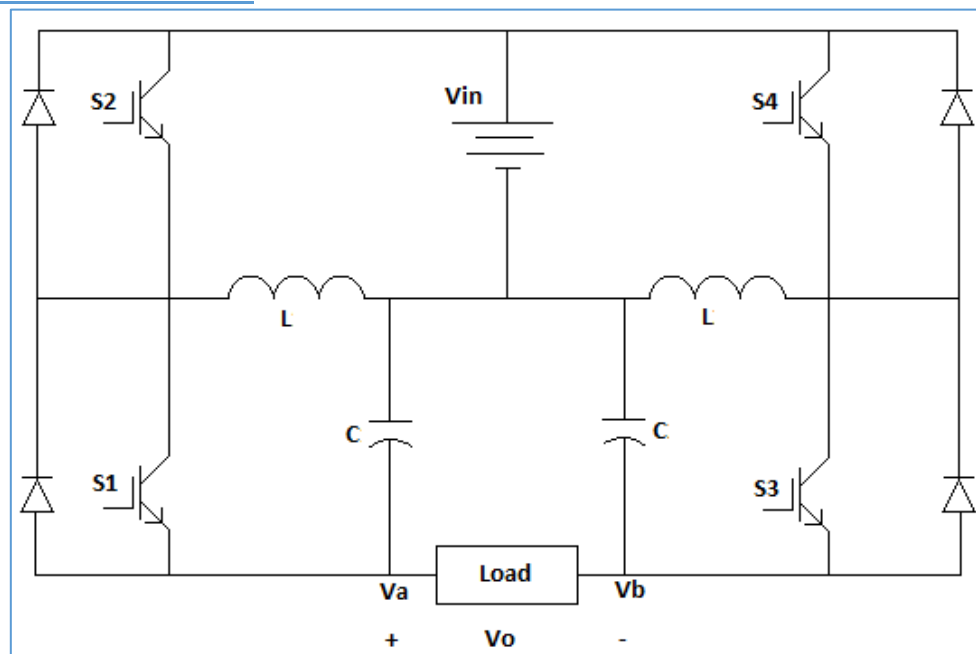
$$D = 0.5 + 0.2 \sin\omega t + 0.01196 \sin 3\omega t$$



**Output voltage of Boost inverter with third harmonic injected duty cycle modulation,**

**Figure 2.9**

### ➤ Buck-Boost inverter



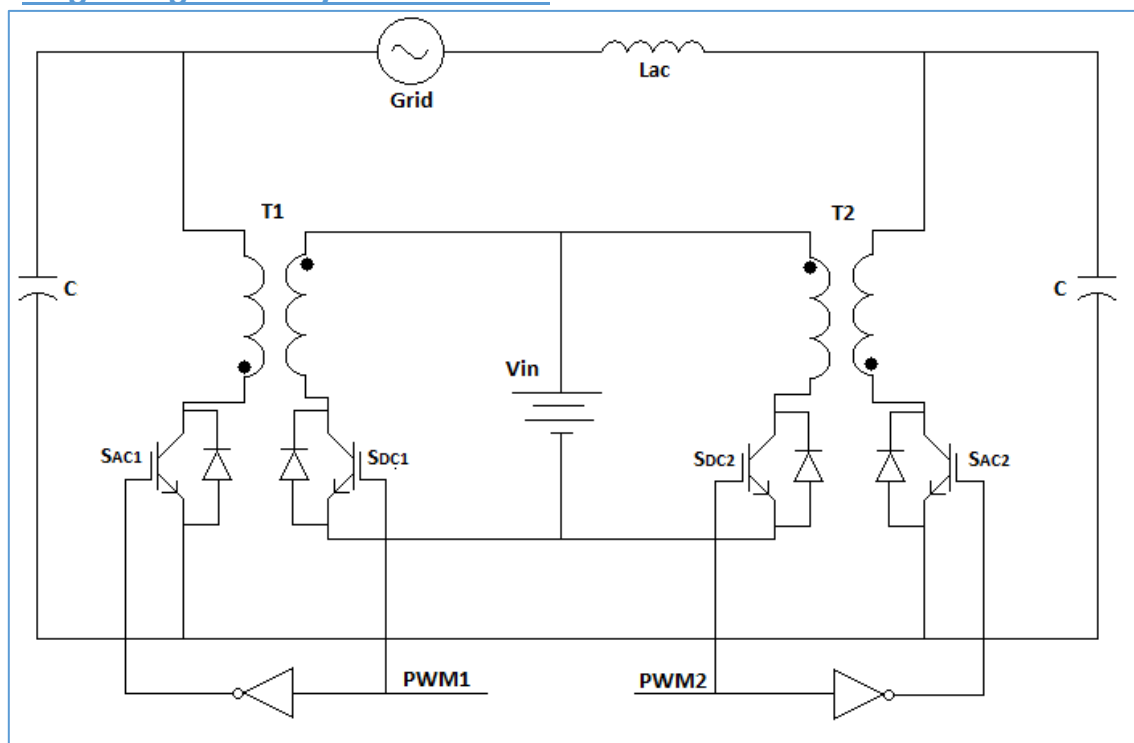
**Buck-boost inverter, Figure 2.10**

The full bridge topology can also be operated as a buck-boost inverter as shown. It almost have same characteristics of boost converter and it can generate an output ac voltage lower or higher than the DC input voltage. Hence, the output voltage of boost inverter is,

$$\begin{aligned}
 V &= V_1 - V_2 \\
 &= \frac{D}{1-D} - \frac{1-D}{D} \\
 &= \frac{(2D-1)}{D(1-D)}
 \end{aligned}$$

At,  $D = 0.5, V = 0$ . If  $D > 0.5, V > 0$  and for  $D < 0.5, V < 0$ .

### ➤ Single stage dual Flyback inverter:

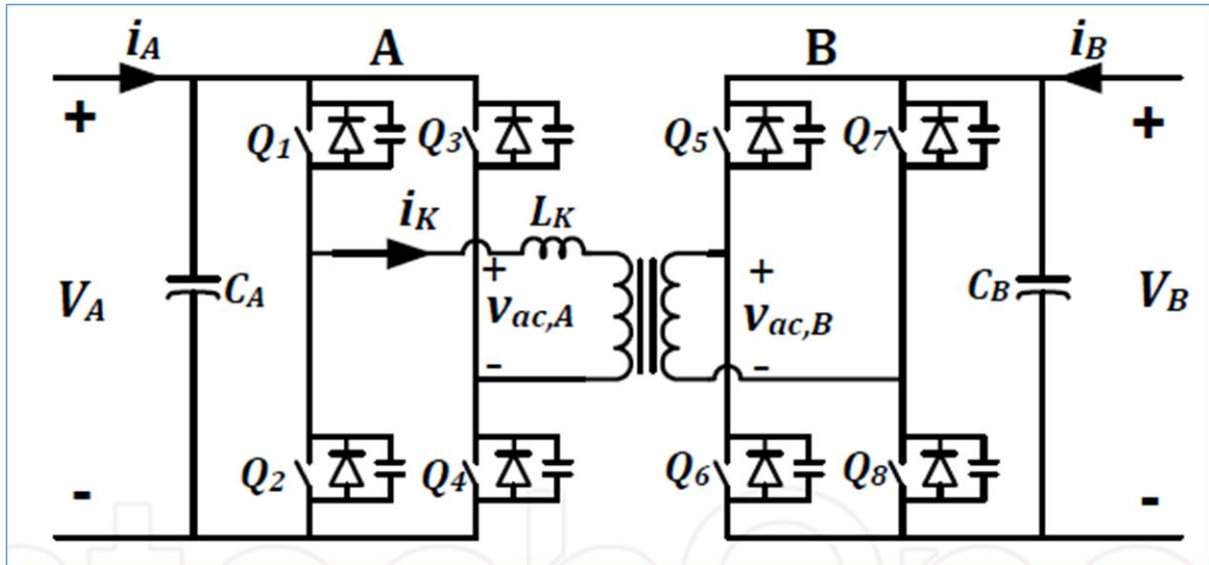


**Single stage dual Flyback inverter, Figure 2.11**

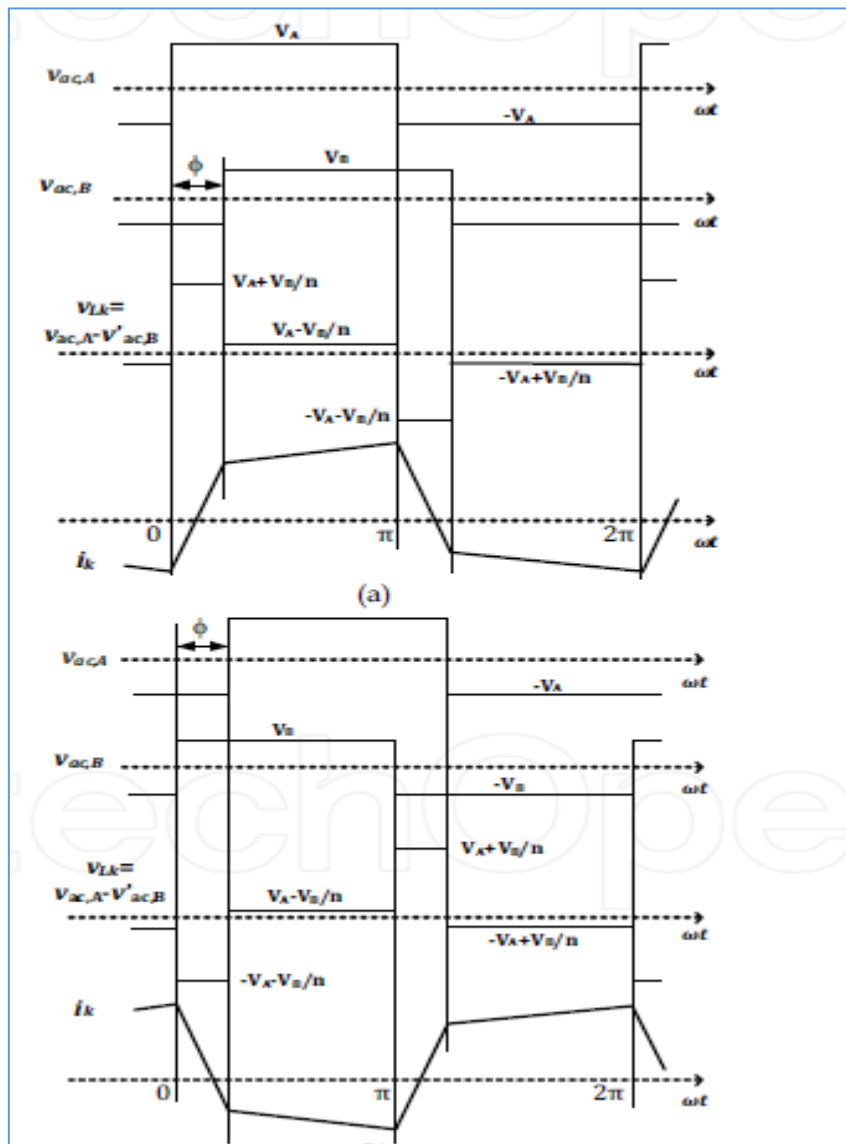
“A novel single-stage inverter for the AC-module with reduced low-frequency ripple penetration” proposed the single stage dual Flyback inverter. In this topology two bidirectional Flyback converters are connected to form main circuit. It provides galvanic isolation by high frequency transformers.

### ➤ Dual active bridge converter with unfold bridge

The converter is introduced in (De Doncker et al., 1991) and (Kheraluwala et al., 1992). In this configuration, full-bridge voltage-fed converters are used at both sides of the isolation transformer and the control is performed based on soft-switched phase-shift strategy. In its basic form, the diagonal switching pairs in each converter are turned on simultaneously with 50% duty cycle (ignoring the small dead time) and with 180 degrees phase shift between two legs to provide a nearly square wave ac voltage across transformer terminals. The phase shift between two ac voltages, denoted by  $\phi$ , is an important parameter which determines the direction and amount of power transfer between dc buses. By adjusting this phase shift, a fixed frequency operation with full control over the power transfer is possible.



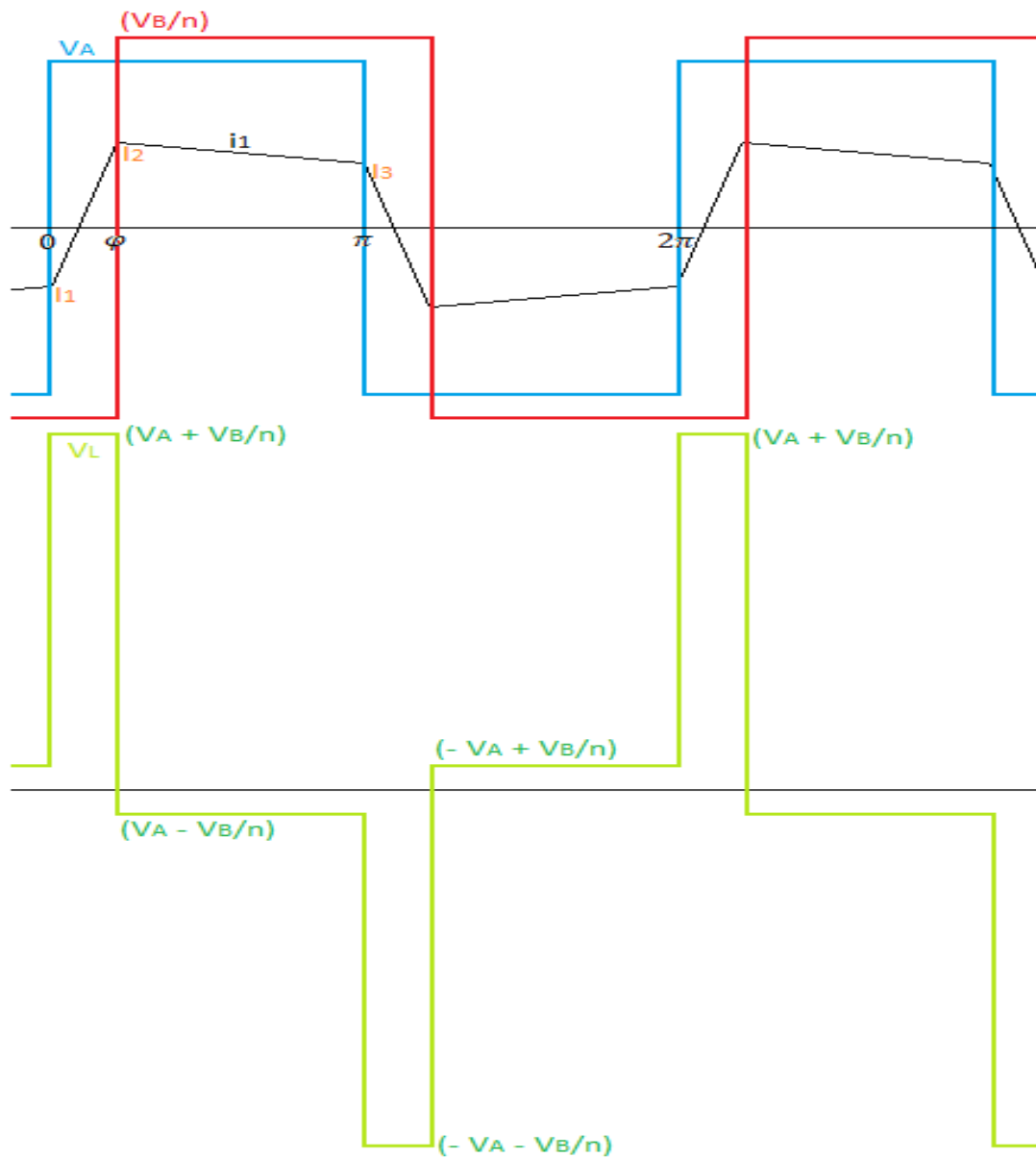
**Circuit diagram of Dual active bridge converter, Figure 2.12**



**Operating waveforms (a) A-to-B mode and (b) B-to-A mode, Figure 2.13**

The average transferred power can be obtained by calculating the average ac power at the transformer terminals, i.e. by using single phase shift modulation (PSM),

### ✓ Calculation of power flow of DAB converter



$$\begin{aligned}
 P &= \frac{1}{2\pi} \int_0^{2\pi} (v_{ac,A} * i_k) d(\omega t) \\
 &= \frac{1}{\pi} \int_0^{\pi} (V_A * i_1) d\theta \\
 &= \frac{V_A}{\pi} \left[ \int_0^{\varphi} i_1 d\theta + \int_{\varphi}^{\pi} i_1 d\theta \right] \dots \dots \dots \text{eqn. 2.1}
 \end{aligned}$$

$$i_1 = I_1 + \left(V_A + \frac{V_B}{n}\right) \frac{1}{2\pi f L_k} \theta; 0 < \theta < \varphi \dots \dots \dots \text{eqn. 2.2}$$

$$= I_2 + \left(V_A - \frac{V_B}{n}\right) \frac{1}{2\pi f L_k} (\theta - \varphi); \varphi < \theta < \pi \dots \dots \dots \text{eqn. 2.3}$$

$f$  is the high switching frequency of the DAB converter.

From half-wave symmetry,  $I_3 = -I_1$

At,  $\theta = \varphi$ ,  $i_1 = I_2$ , hence, from eqn. 2.2,

$$I_2 = I_1 + \left(V_A + \frac{V_B}{n}\right) \frac{1}{2\pi f L_k} \varphi \dots \dots \dots \text{eqn. 2.4}$$

At,  $\theta = \pi$ ,  $i_1 = I_3$ , hence, from eqn. 2.3,

$$I_3 = I_2 + \left(V_A - \frac{V_B}{n}\right) \frac{1}{2\pi f L_k} (\pi - \varphi)$$

$$-I_1 = I_1 + \left(V_A + \frac{V_B}{n}\right) \frac{1}{2\pi f L_k} \varphi + \left(V_A - \frac{V_B}{n}\right) \frac{1}{2\pi f L_k} (\pi - \varphi); \text{ ( Putting } I_3 = -I_1 \text{)}$$

$$I_1 = \left[ \frac{V_B}{n} \left( \frac{\pi}{2} - \varphi \right) - V_A \left( \frac{\pi}{2} \right) \right] \left( \frac{1}{2\pi f L_k} \right) \dots \dots \dots \text{eqn. 2.5}$$

Hence, putting the value of eqn. 2.5 in eqn. 2.4,

$$I_2 = \left[ \frac{V_B}{n} \left( \frac{\pi}{2} - \varphi \right) - V_A \left( \frac{\pi}{2} \right) \right] \left( \frac{1}{2\pi f L_k} \right) + \left( V_A + \frac{V_B}{n} \right) \left( \frac{1}{2\pi f L_k} \right) \varphi$$

$$I_2 = \left[ \frac{V_B \pi}{2n} - \frac{V_A \pi}{2} + V_A \varphi \right] \left( \frac{1}{2\pi f L_k} \right) \dots \dots \dots \text{eqn. 2.6}$$

Putting the value of  $i_1$  from eqn. 2.2 & eqn. 2.3 in eqn. 2.1,

$$P_{avg} = \frac{V_A}{\pi} \left[ \int_0^\varphi \left[ I_1 + \left( V_A + \frac{V_B}{n} \right) \frac{1}{2\pi f L_k} \theta \right] d\theta + \int_\varphi^\pi \left[ I_2 + \left( V_A - \frac{V_B}{n} \right) \frac{1}{2\pi f L_k} (\theta - \varphi) \right] d\theta \right]$$

$$= \frac{V_A}{\pi} \left[ \left[ I_1 \varphi + \left( V_A + \frac{V_B}{n} \right) \frac{1}{2\pi f L_k} \frac{\varphi^2}{2} \right] + \left[ I_2 (\pi - \varphi) + \left( V_A - \frac{V_B}{n} \right) \frac{1}{2\pi f L_k} \frac{(\pi - \varphi)^2}{2} \right] \right]$$

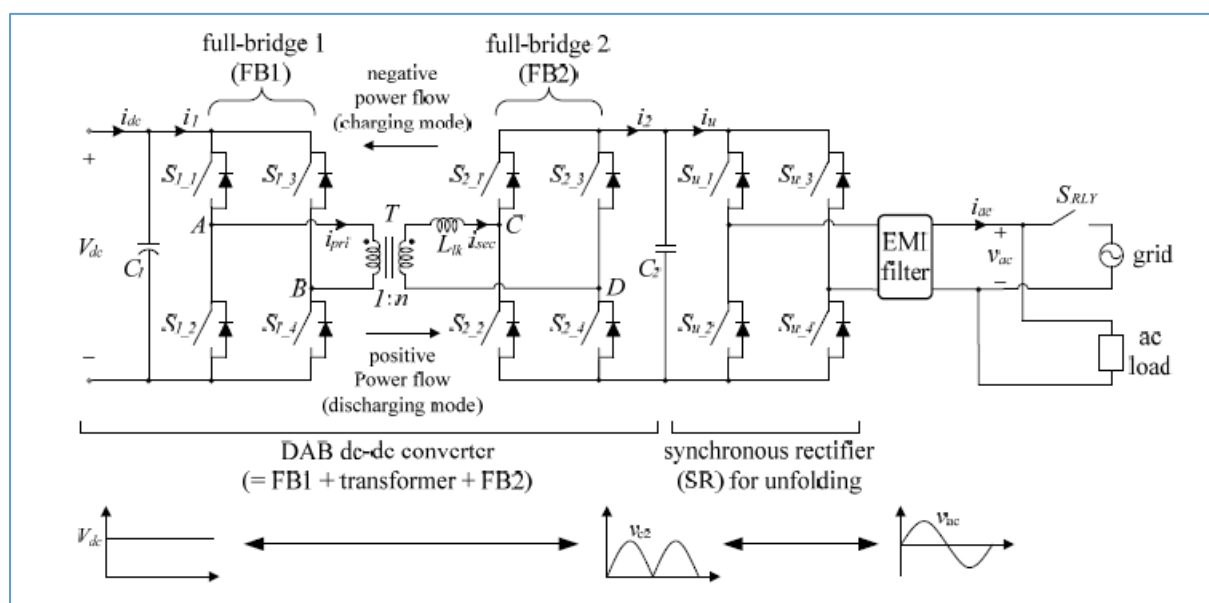
Putting the value of  $I_1$  &  $I_2$  from eqn. 2.5 & eqn. 2.6 in the above equation and simplifying we get,

$$P_{avg} = \frac{V_A V_B \varphi (\pi - \varphi)}{2\pi^2 L_k n f} \dots \dots \dots \text{eqn. 2.7}$$

Where  $L_k$  is the transformer leakage inductance (plus any series inductance),  $n$  is the transformer turns ratio (Side B to Side A) and  $\omega$  is the angular frequency. To transfer power from Side A to Side B (A-to-B mode),  $v_{ac,A}$  should lead  $v_{ac,B}$  and  $\varphi$  is considered as positive. In B-to-A mode,  $v_{ac,A}$  should lag  $v_{ac,B}$  and  $\varphi$  is negative. This leading or lagging phase shift is simply implemented by proper timing control of converter switches.  $L_k$  is an important element which determines the maximum amount of transferable power with given switching frequency. Therefore, apart from other practical limitations, it is possible to reach a high power density converter with a low leakage transformer.

There are several other types of modulation techniques based on both phase shift control and duty ratio control such as Trapezoidal modulation (TPZM), Triangular modulation (special case of TPZM), hybrid of PSM, TPZM or TRM can be used for control of Dual active bridge converter.

By using variable frequency control in hybrid modulation technique, Since  $i_u$  is directly proportional to  $\varphi$  when using the hybrid modulation, the phase shift angle  $\varphi$  should be a rectified sine wave in phase with  $i_{ac}$  as a following function  $\varphi(t)$  to achieve unity power factor we can get perfect sinusoid grid current which in turn creates a rectified sinusoid dc link voltage which can be unfolded by Unfolder Bridge as per the paper "High-efficiency Bidirectional DAB Inverter using a Novel Hybrid Modulation for Stand-alone Power Generating System with Low Input Voltage".

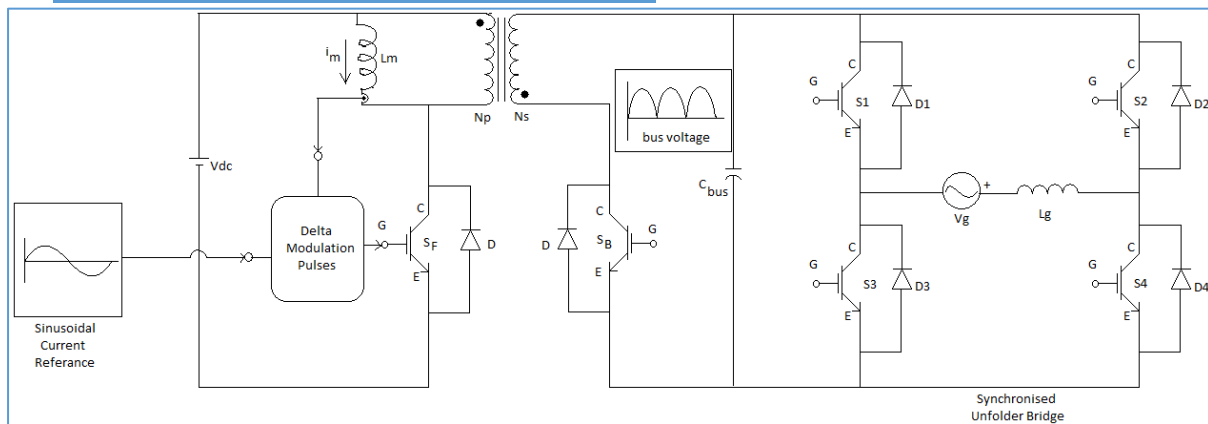


**Bidirectional DAB inverter for the stand-alone generating system with single power-conversion stage, Figure 2.14**

For high input voltage and output voltage ratio, transformerless configuration is not suited as it cannot provide galvanic isolation. Therefore, Dual active bridge inverter and buck-boost converter derived Flyback inverter are widely used. Apart from that DAB has only step down function. Thus it requires high transformer turns ratio to achieve voltage matching to grid level. But Flyback converter can both step up and step down.



### ➤ Flyback converter with unfolder bridge



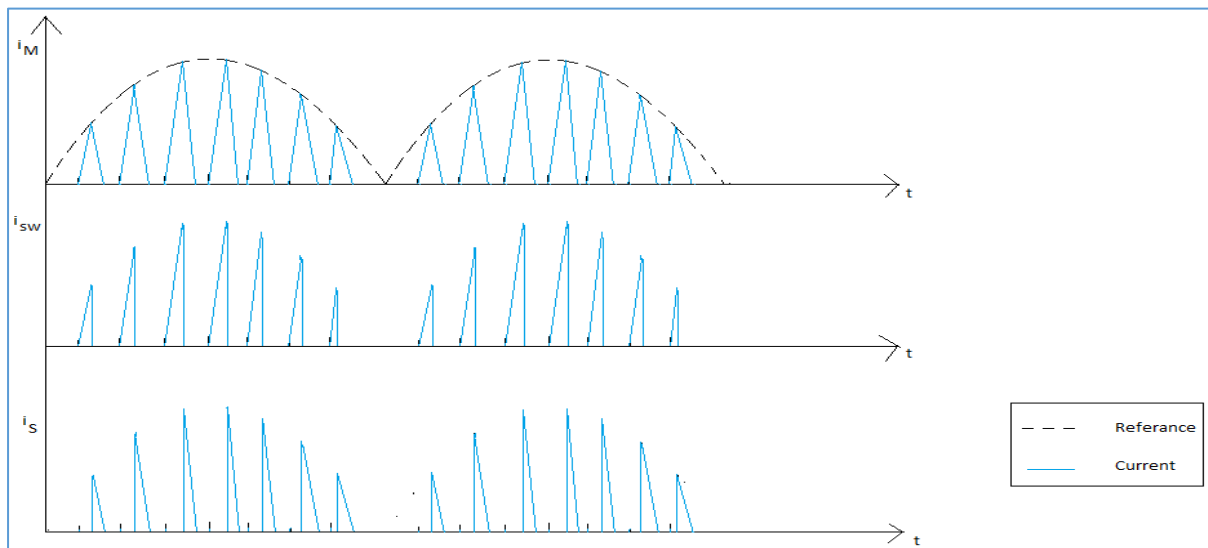
**Circuit Diagram of Flyback converter with unfolder bridge, Figure 2.15**

Single stage inverter is used for single stage dc to ac power conversion for better efficiency. The main aim is to inject sinusoidal current wave form to grid. For sinusoidal current waveform, the current through magnetizing inductance is shaped in the form of rectified sinusoid by comparing the  $i_m$  with rectified sinusoidal current reference signal. Flyback converter is derived from buck-boost chopper. Buck-boost chopper can be operated in both continuous and discontinuous conduction mode. But discontinuous conduction mode is preferred over continuous conduction mode because of need of smaller magnetizing inductance has quicker response and lower transient output voltage spike to sudden change in load current or input voltage. Apart from that, from state space averaged model of both boost and buck-boost chopper in continuous conduction mode has a right half plane zero in the transfer function of loop gain which creates an initial drop of output voltage for an incremental step change in duty cycle and thus require more difficult feedback control circuit to eliminate that right half plane zero. But for high power application Flyback converter has to be operated in continuous conduction mode. Due to rectified sinusoid nature of dc bus voltage requires a lower valued dc bus capacitance just to eliminate higher order harmonics of dc link current which is another advantage of Single-stage inverter. That filtered dc link current is unfolded by using synchronised unfolder bridge. The secondary side switch is operated at high frequency to transfer power from grid to dc source. Thus this converter offers bidirectional power flow.

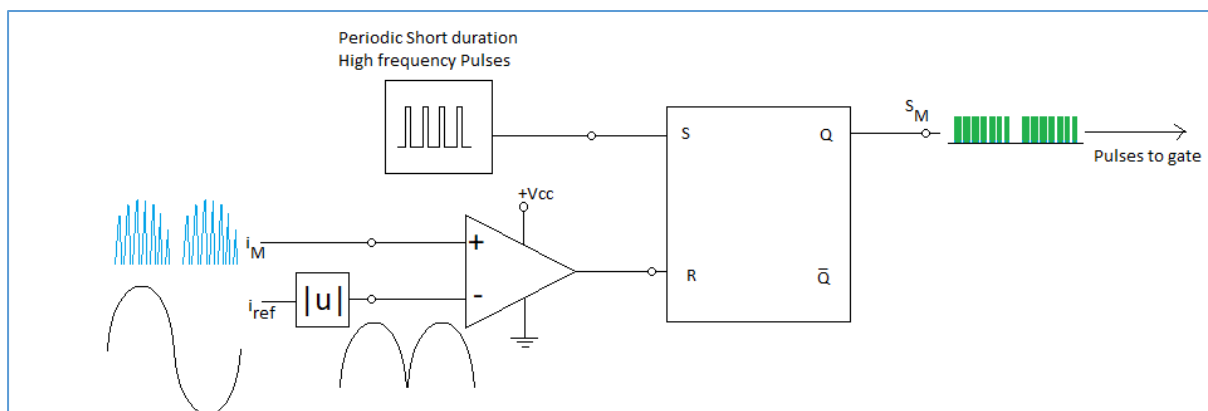
Later in this thesis we have concentrated on Flyback converter driven single-stage inverter.

## CHAPTER-3

### Circuit operation with current mode control

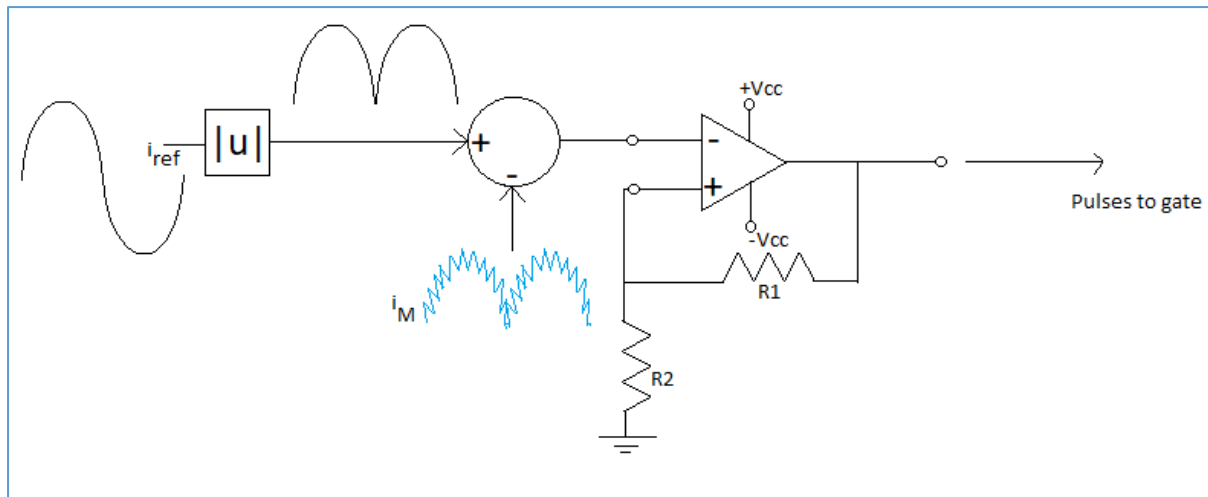


**Magnetizing Inductor Current, Primary Switch current and dc link current respectively at DCM, Figure 3.1**



**Gate switching pulse generation block diagram, Figure 3.2**

For creating rectified sinusoidal magnetizing inductance current this current is compared with a rectified sinusoid and the comparator output is zero when  $i_M$  is less than the rectified sinusoidal reference current, thus R is at zero. When a pulse appears at S of S-R flip-flop, for  $S=1$  and  $R=0$  sets the S-R flip-flop making the switch on and the inductor current continues to increase linearly for input voltage until it reaches the sinusoidal reference. When  $i_M$  tries to increase beyond the reference, comparator output becomes one. So R is at one. For  $S=0$  and  $R=1$ , S-R flip-flop resets, thus  $Q=0$  making the switch off. Inductor current starts to decay until the second pulse appears at S. If the pulse frequency is very high, the Flyback inverter operates at continuous conduction mode. If pulse frequency is lower than discharging rate of magnetizing inductance current, Flyback converter operates at discontinuous conduction mode. Thus by varying the pulse frequency, we can operate the Flyback inverter at continuous or discontinuous conduction mode.

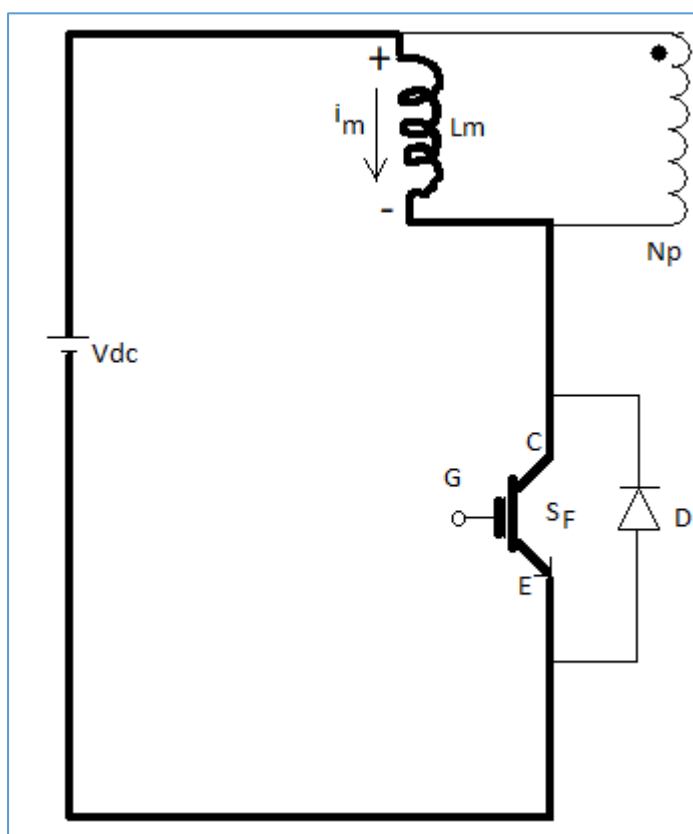


**Hysteresis band current controller for gate pulse generation, Figure 3.3**

Another way to shape the inductor current is by using hysteresis band current controller. When the current exceeds the hysteresis band, the comparator output becomes low thus making the switch off, inductor current starts to decay. When the current crosses the lower band limit, the comparator output becomes high and switch becomes on and the inductor current again increases. In this way the inductor current is forced to track the sinusoidal reference. This type of control gives CCM operation and high quality grid current.

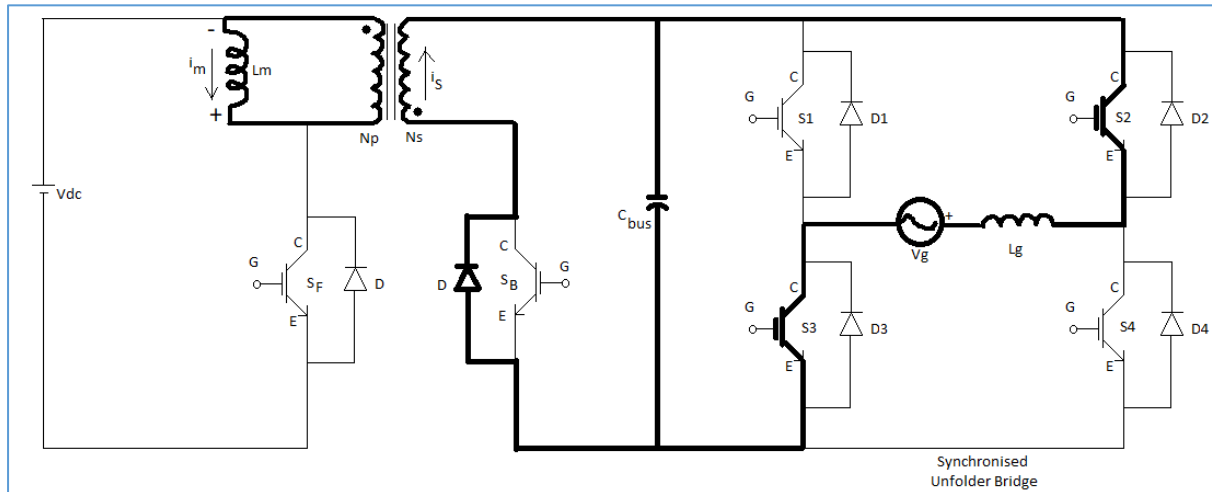
- **Discharging Mode**

**Mode1: S<sub>F</sub> Switch is ON**



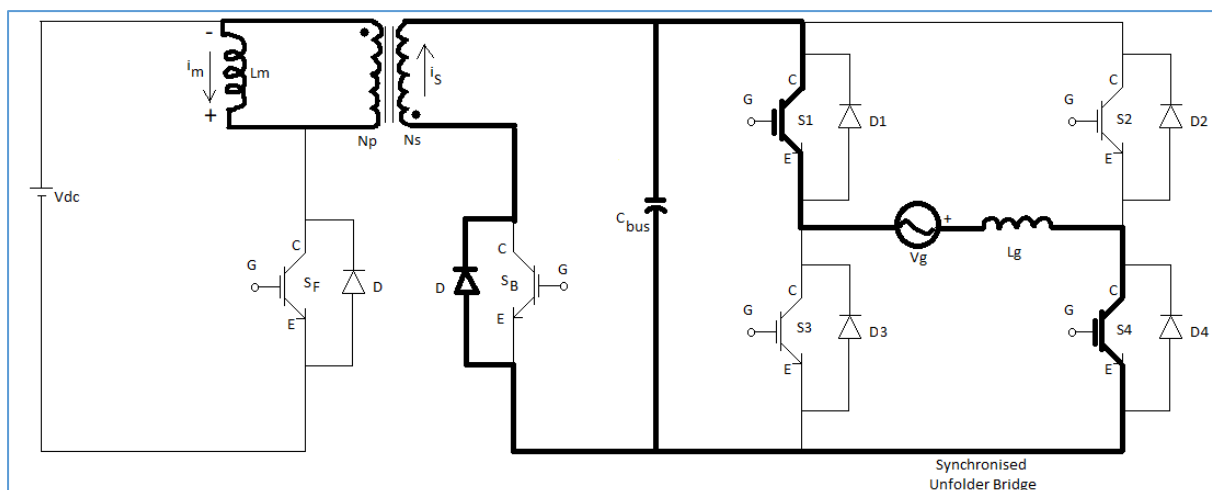
When the switch is on, the inductor current starts to increase through the switch until it reaches the reference current. In this duration of time inductor stores energy with upper polarity positive and lower polarity negative and no current flows to the secondary as secondary side diode is in reverse biased condition.

### Mode2A: $S_F$ Switch is OFF, S2, S3 ON (grid Voltage +ve Half Cycle)



When inductor current reaches the reference current the switch becomes off and the polarity of inductor reverses thus the stored energy transfers to the secondary side through the transformer and the secondary side current flows to the grid through the unfold-bridge and forward biased antiparallel diode of secondary side switch. **Mode1 and Mode2A will continue cyclically at switching frequency in positive half cycle of grid voltage.**

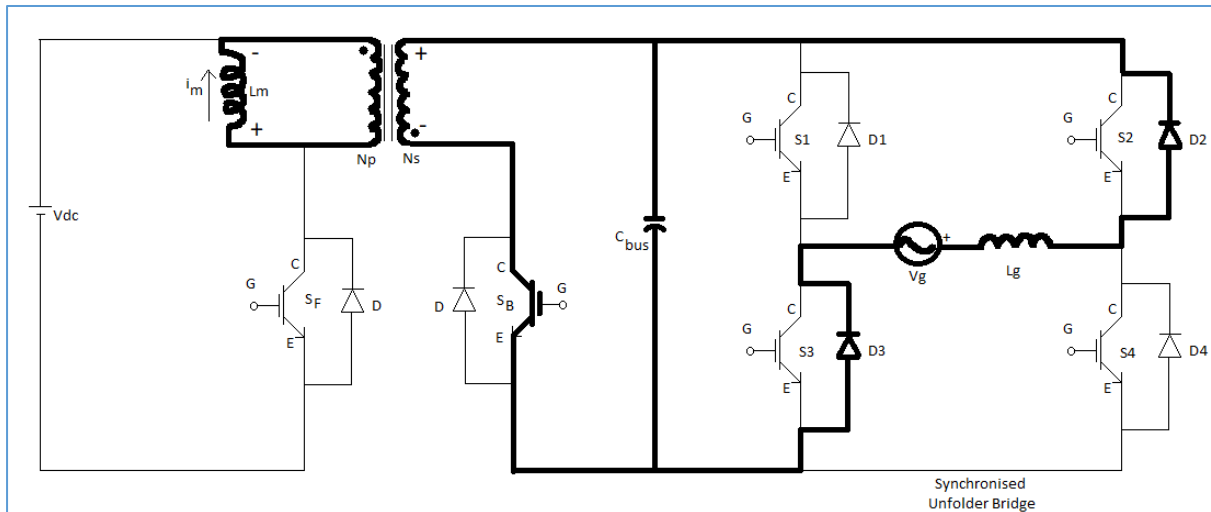
### Mode2B: $S_F$ Switch is OFF, S1, S4 ON (grid Voltage -ve Half Cycle)



**Similarly Mode1 and Mode2B will continue cyclically at switching frequency in negative half cycle of grid voltage.**

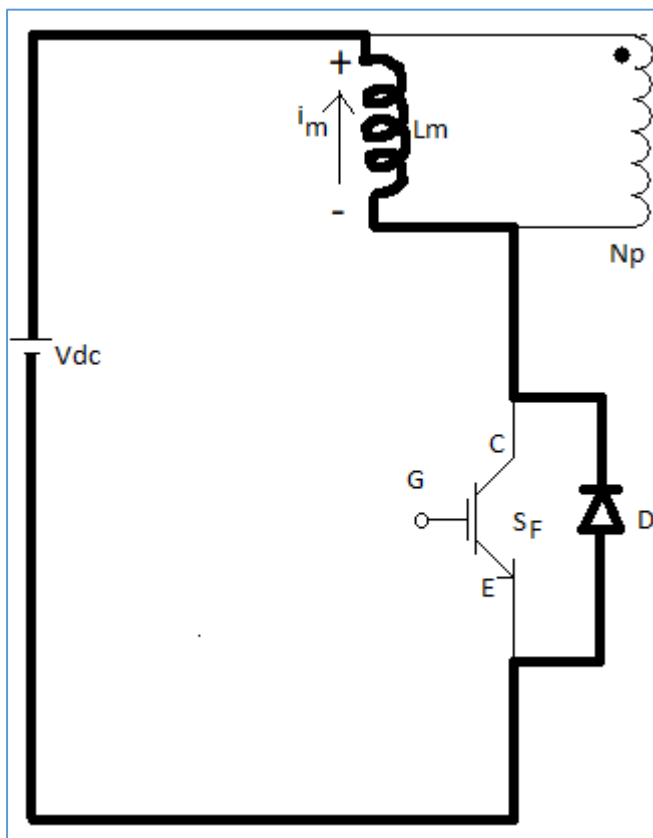
- Charging Mode

### Mode 1: $S_B$ Switch is ON



When the secondary switch is on and all switching pulses of the unfold circuit is absent, the unfold bridge acts as a full wave bridge rectifier with antiparallel diodes D1, D2, D3 & D4. The magnetizing inductance charges by grid voltage with the polarity as shown.

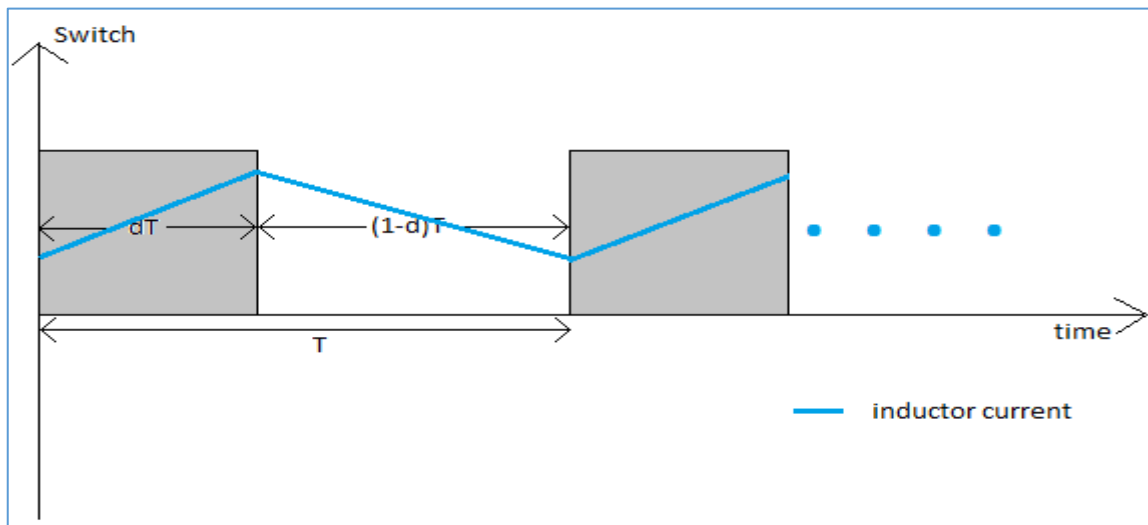
### Mode 2: $S_B$ Switch is OFF



When the secondary side switch is off, the stored energy of inductor is fed to the dc supply through antiparallel diode of the primary side switch. **Mode1 and Mode2 will continue cyclically at switching frequency.**

## CHAPTER- 4

### State Space Averaging in CCM:



**Switching sequence diagram, Figure 4.1**

#### Interval $dT$ :

$$\dot{x} = A_1 x + b_1 v_g \dots \dots \dots \text{eqn. 4.1.1}$$

$$y_1 = C_1^T x \dots \dots \dots \text{eqn. 4.1.2}$$

#### Interval $(1-d)T$ :

$$\dot{x} = A_2 x + b_2 v_g \dots \dots \dots \text{eqn. 4.2.1}$$

$$y_2 = C_2^T x \dots \dots \dots \text{eqn. 4.2.2}$$

From eqn. 4.1.1 & eqn. 4.2.1 for Linear Continuous system, state space averaged expression of state variables is,

$$\dot{x} = d(A_1 x + b_1 v_g) + d'(A_2 x + b_2 v_g) \dots \dots \dots \text{eqn. 4.3.1}$$

Similarly from eqn. 4.1.2 & eqn. 4.2.2,

$$y = d y_1 + d' y_2$$

$$= (d C_1^T + d' C_2^T) x \dots \dots \dots \text{eqn. 4.3.2}$$

Where  $A_1, b_1$  &  $A_2, b_2$  are equivalent state matrices in each interval respectively and " $x$ " is the matrix of state variables and " $y$ " is the output matrix and  $d' = (1 - d)$ . Here duty cycle " $d$ " and input voltage " $v_g$ " are constant. Following is the overall state space averaged expression.

Rearranging terms in eqn. 4.3.1 & eqn. 4.3.2 we get,

$$\dot{x} = A x + b v_g \dots \dots \dots \text{eqn. 4.4.1}$$

$$y = C^T x \dots \dots \dots \text{eqn. 4.4.2}$$

These are the overall equations where

$$A = d A_1 + d' A_2, b = d b_1 + d' b_2, C^T = d C_1^T + d' C_2^T$$

**Perturbation:** There are two types of perturbations [1. Line Voltage variation](#), [2. Duty cycle variation](#).

### 1. Line Voltage Variation:

$$\text{For, } v_g = V_g + \widehat{v_g}$$

$$x = X + \widehat{x} \text{ \& } y = Y + \widehat{y}$$

Hence, putting x and y in *eqn. 4.4.1* & *eqn. 4.4.2*, we get,

$$\dot{X} + \dot{\widehat{x}} = A (X + \widehat{x}) + b (V_g + \widehat{v_g}) \dots \dots \dots \text{eqn. 4.5.1}$$

$$(Y + \widehat{y}) = C^T X + C^T \widehat{x} \dots \dots \dots \text{eqn. 4.5.2}$$

**Separation of steady state (d.c) part from dynamic (a.c) part:**

#### a) D.C Model:

From *eqn. 4.5.1*, separating D.C part we get,

$$A X + b V_g = 0 \text{ (As at steady state, } \dot{X} = 0)$$

$$\Rightarrow X = -(A^{-1} b V_g) \dots \dots \dots \text{eqn. 4.6.1}$$

Similarly from *eqn. 4.5.2*, separating D.C part we get,

$$Y = C^T X$$

$$\Rightarrow Y = -C^T A^{-1} b V_g \dots \dots \dots \text{eqn. 4.6.2}$$

#### b) Dynamic (a.c) model:

From *eqn. 4.5.1* & *eqn. 4.5.2*, separating A.C part we get,

$$\dot{\widehat{x}} = A \widehat{x} + b \widehat{v_g} \dots \dots \dots \text{eqn. 4.7.1}$$

$$\widehat{y} = C^T \widehat{x} \dots \dots \dots \text{eqn. 4.7.2}$$

### 2. Duty cycle variation:

$$d = D + \widehat{d}; d' = (1 - d) = (1 - D) - \widehat{d} = D' - \widehat{d}$$

Now considering the total perturbation i.e. both line voltage variation and duty cycle variation from *eqn. 4.7.1* & *eqn. 4.7.2* we get,

$$\begin{aligned} \dot{x} &= [(D + \widehat{d}) A_1 + (D' - \widehat{d}) A_2] (X + \widehat{x}) + [(D + \widehat{d}) b_1 + (D' - \widehat{d}) b_2] (V_g + \widehat{v_g}) \\ &= [(D A_1 X + D' A_2 X) + (\widehat{d} A_1 X - \widehat{d} A_2 X)] + [(D A_1 \widehat{x} + D' A_2 \widehat{x}) + (\widehat{d} A_1 \widehat{x} - \widehat{d} A_2 \widehat{x})] \\ &\quad + [(D b_1 V_g + D' b_2 V_g) + (\widehat{d} b_1 V_g - \widehat{d} b_2 V_g)] + [(D b_1 \widehat{v_g} + D' b_2 \widehat{v_g}) + (\widehat{d} b_1 \widehat{v_g} - \widehat{d} b_2 \widehat{v_g})] \end{aligned}$$

$$\begin{aligned} \dot{x} &= (A X + b V_g) + (A \widehat{x} + b \widehat{v_g}) + [(A_1 - A_2) X + (b_1 - b_2) V_g] \widehat{d} \\ &\quad + [(A_1 - A_2) \widehat{x} + (b_1 - b_2) \widehat{v_g}] \widehat{d} \dots \dots \dots \text{eqn. 4.8.1} \end{aligned}$$

$$y = [(D + \hat{d}) C_1^T + (D' - \hat{d}) C_2^T] (X + \hat{x})$$

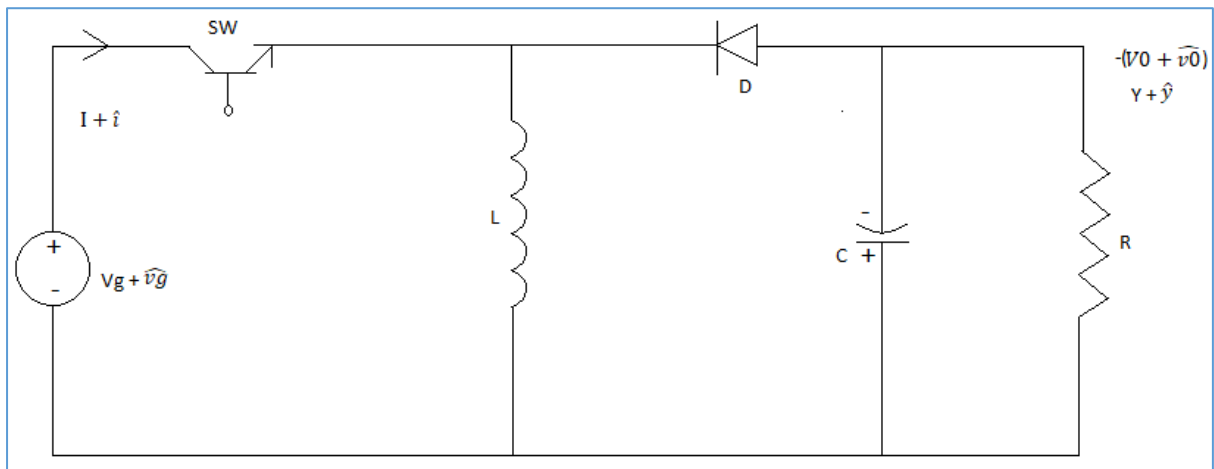
$$= (D C_1^T X + D' C_2^T X) + (\hat{d} C_1^T X - \hat{d} C_2^T X) + (D C_1^T \hat{x} + D' C_2^T \hat{x})$$

$$+ (\hat{d} C_1^T \hat{x} - \hat{d} C_2^T \hat{x})$$

$$y = C^T X + C^T \hat{x} + (C_1^T - C_2^T) X \hat{d} + (C_1^T - C_2^T) \hat{x} \hat{d} \dots \dots \dots \text{eqn. 4.8.2}$$

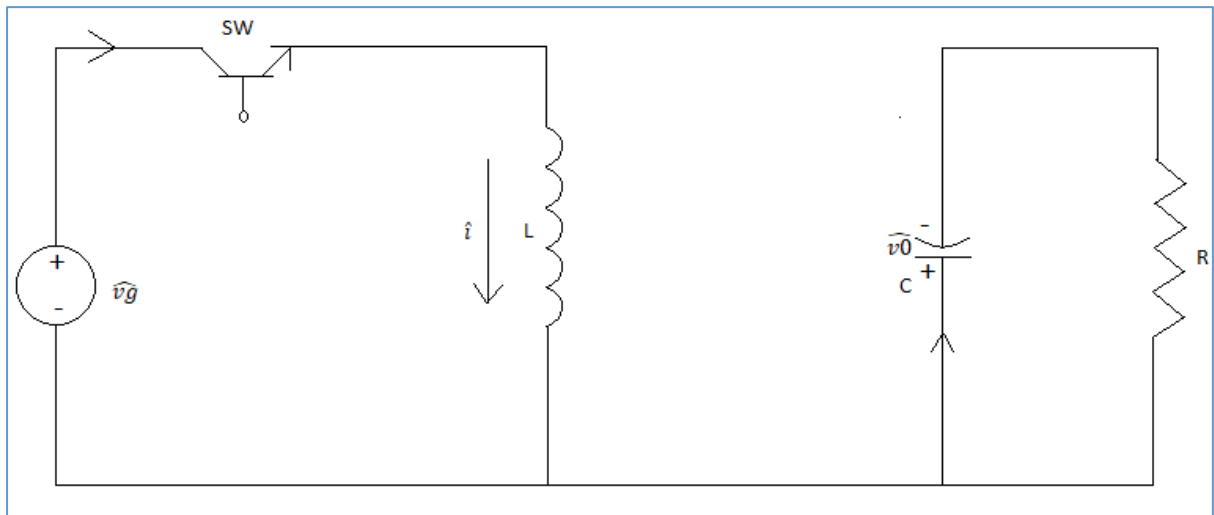
• **State Space averaging of Buck-Boost converter (at CCM)**

Ignoring equivalent series resistance of capacitor and equivalent series resistance of inductor following is the model of buck-boost converter.



A.C Model analysis:

Switch ON duration:



$$\hat{v}_g = L \hat{i}$$

$$\Rightarrow \hat{i} = \left(\frac{1}{L}\right) \hat{v}_g$$

$$-C \dot{v} R = v, \text{ (Taking, } v = \hat{v}_0 \text{.)}$$



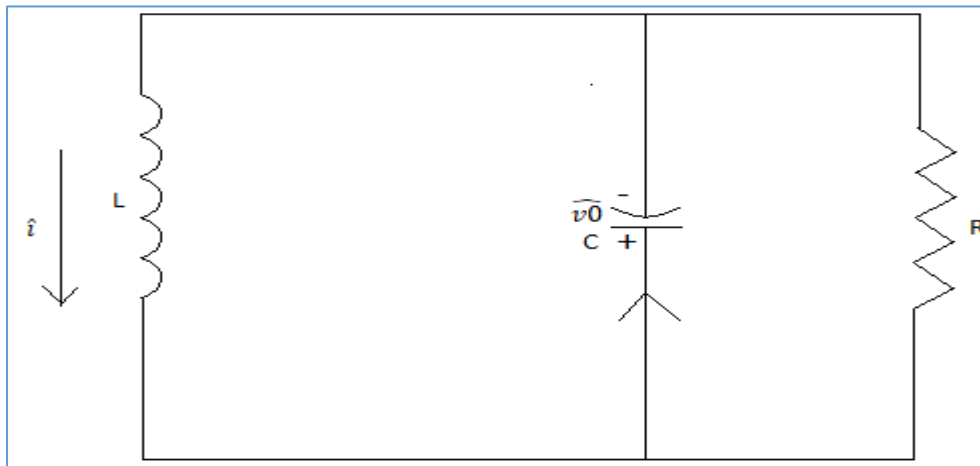
$$\Rightarrow \dot{v} = \left(-\frac{1}{RC}\right) v$$

Hence in matrix form:

$$\begin{bmatrix} \dot{i} \\ \dot{v} \end{bmatrix} = \begin{bmatrix} 0 & 0 \\ 0 & \left(-\frac{1}{RC}\right) \end{bmatrix} \begin{bmatrix} \hat{i} \\ v \end{bmatrix} + \begin{bmatrix} \left(\frac{1}{L}\right) \\ 0 \end{bmatrix} \widehat{v}g \dots \dots \dots \text{eqn. 4.9.1}$$

$\mathbf{A}_1 \qquad \mathbf{b}_1$

Switch OFF duration:



$$-L \dot{i} = v$$

$$\Rightarrow \dot{i} = -\left(\frac{1}{L}\right) v$$

$$v = iR - C\dot{v}$$

$$\Rightarrow \dot{v} = \left(\frac{1}{C}\right) i - \left(\frac{1}{RC}\right) v$$

Hence in matrix form:

$$\begin{bmatrix} \dot{i} \\ \dot{v} \end{bmatrix} = \begin{bmatrix} 0 & \left(-\frac{1}{L}\right) \\ \left(\frac{1}{C}\right) & \left(-\frac{1}{RC}\right) \end{bmatrix} \begin{bmatrix} \hat{i} \\ v \end{bmatrix} + \begin{bmatrix} 0 \\ 0 \end{bmatrix} \widehat{v}g \dots \dots \dots \text{eqn. 4.9.2}$$

$\mathbf{A}_2 \qquad \mathbf{b}_2$

Hence the overall state space averaged matrix representation considering duty ratio variation and ignoring nonlinear higher order terms from eqn. 4.8.1, eqn. 4.9.1 & eqn. 4.9.2, we get,

$$\begin{bmatrix} \dot{i} \\ \dot{v} \end{bmatrix} = \begin{bmatrix} 0 & \left(-\frac{D'}{L}\right) \\ \left(\frac{D'}{C}\right) & \left(-\frac{1}{RC}\right) \end{bmatrix} \begin{bmatrix} \hat{i} \\ v \end{bmatrix} + \begin{bmatrix} \left(\frac{D}{L}\right) \\ 0 \end{bmatrix} \widehat{v}g + [(A_1 - A_2) X + (b_1 - b_2) Vg] \hat{d} \dots \dots \dots \text{eqn. 4.10.1}$$

$\mathbf{A} \qquad \mathbf{b} \qquad \text{(Duty ratio variation term)}$

$$\hat{y} = [0 \quad -1] \begin{bmatrix} \hat{i} \\ v \end{bmatrix} \dots \dots \dots \text{eqn. 4.10.2}$$

$\mathbf{C}^T$

### D.C Model analysis:

$A X + b Vg = 0$  (As  $\dot{X} = 0$  at steady state for d.c term)

$$\Rightarrow X = -(A^{-1}b Vg) \dots \dots \dots \text{eqn. 4.11}$$

Hence, putting the value of eqn. 4.11 on duty ratio variation term of eqn. 4.10.1 we get,

$$= [(A_1 - A_2) \{-(A^{-1}b Vg)\} + (b_1 - b_2) Vg] \hat{d}$$

$$= [-(A_1 - A_2) (A^{-1}b) + (b_1 - b_2)] Vg \hat{d} \dots \dots \dots \text{eqn. 4.12}$$

$$(A_1 - A_2) = \begin{bmatrix} 0 & \left(-\frac{1}{L}\right) \\ \left(\frac{1}{C}\right) & 0 \end{bmatrix}$$

$$A^{-1} = \left(\frac{LC}{D'^2}\right) \begin{bmatrix} \left(-\frac{1}{RC}\right) & \left(\frac{D'}{L}\right) \\ \left(-\frac{D'}{C}\right) & 0 \end{bmatrix}$$

$$A^{-1}b = \left(\frac{LC}{D'^2}\right) \begin{bmatrix} \left(-\frac{D}{RLC}\right) \\ \left(-\frac{DD'}{LC}\right) \end{bmatrix}$$

$$Y = C^T X$$

$$Y = C^T \left(\frac{LC}{D'^2}\right) \begin{bmatrix} \left(-\frac{D}{RLC}\right) \\ \left(-\frac{DD'}{LC}\right) \end{bmatrix} Vg$$

$$= -[0 \quad -1] \left(\frac{LC}{D'^2}\right) \begin{bmatrix} \left(-\frac{D}{RLC}\right) \\ \left(-\frac{DD'}{LC}\right) \end{bmatrix} Vg$$

$$= -\left(\frac{DVg}{D'}\right)$$

Hence,

$$V_o = \left(\frac{DVg}{D'}\right) \dots \dots \dots \text{eqn. 4.13}$$

Now,

$$\begin{aligned}
 & (A_1 - A_2) (A^{-1}b) \\
 &= \left(\frac{LC}{D'^2}\right) \begin{bmatrix} 0 & \left(-\frac{1}{L}\right) \\ \left(\frac{1}{C}\right) & 0 \end{bmatrix} \begin{bmatrix} \left(-\frac{D}{RLC}\right) \\ \left(-\frac{DD'}{LC}\right) \end{bmatrix} \\
 &= \left(\frac{LC}{D'^2}\right) \begin{bmatrix} \left(-\frac{DD'}{L^2C}\right) \\ \left(-\frac{D}{RLC^2}\right) \end{bmatrix} \dots \dots \dots \text{eqn. 4.14.1}
 \end{aligned}$$

$$(b_1 - b_2) = \begin{bmatrix} \left(\frac{1}{L}\right) \\ 0 \end{bmatrix} \dots \dots \dots \text{eqn. 4.14.2}$$

Hence, putting eqn. 4.14.1 & eqn. 4.14.2 in eqn. 4.12 we get,

$$\begin{aligned}
 & [-(A_1 - A_2) (A^{-1}b) + (b_1 - b_2)]Vg \hat{d} \\
 &= \left\{ -\left(\frac{LC}{D'^2}\right) \begin{bmatrix} \left(-\frac{DD'}{L^2C}\right) \\ \left(-\frac{D}{RLC^2}\right) \end{bmatrix} + \begin{bmatrix} \left(\frac{1}{L}\right) \\ 0 \end{bmatrix} \right\} Vg \hat{d} \\
 &= \begin{bmatrix} \left(\left(\frac{D}{D'L}\right) + \left(\frac{1}{L}\right)\right) \\ \left(-\frac{D}{D'^2RC}\right) \end{bmatrix} Vg \hat{d}
 \end{aligned}$$

Hence the duty ratio variation term is

$$\begin{bmatrix} \left(\left(\frac{D}{D'L}\right) + \left(\frac{1}{L}\right)\right) \\ \left(-\frac{D}{D'^2RC}\right) \end{bmatrix} Vg \hat{d} = \begin{bmatrix} \left(\left(\frac{V_o}{L}\right) + \left(\frac{V_g}{L}\right)\right) \\ \left(-\frac{V_o}{D'RC}\right) \end{bmatrix} \hat{d} \quad (\text{As } V_o = \left(\frac{DV_g}{D'}\right))$$

**Note:** In case of continuous conduction mode dc gain  $\left(\frac{V_o}{V_g}\right)$  is only dependent on duty ratio and resistances in original model because it is the solution of linear system of equations. It does not depend on storage elements L and C.

Hence, from eqn. 4.10.1, we get,

$$\begin{bmatrix} \dot{i} \\ \dot{v} \end{bmatrix} = \begin{bmatrix} 0 & \left(-\frac{D'}{L}\right) \\ \left(\frac{D'}{C}\right) & \left(-\frac{1}{RC}\right) \end{bmatrix} \begin{bmatrix} i \\ v \end{bmatrix} + \begin{bmatrix} \left(\frac{D}{L}\right) \\ 0 \end{bmatrix} \widehat{v_g} + \begin{bmatrix} \left(\left(\frac{V_o}{L}\right) + \left(\frac{V_g}{L}\right)\right) \\ \left(-\frac{V_o}{D'RC}\right) \end{bmatrix} \hat{d} \dots \dots \dots \text{eqn. 4.15}$$

- Transfer function analysis:

Doing Laplace transform in eqn. 4.15, the state space matrix is as follows

$$s \begin{bmatrix} \hat{i}(s) \\ \hat{v}(s) \end{bmatrix} = \begin{bmatrix} 0 & \left(-\frac{D'}{L}\right) \\ \left(\frac{D'}{C}\right) & \left(-\frac{1}{RC}\right) \end{bmatrix} \begin{bmatrix} \hat{i}(s) \\ \hat{v}(s) \end{bmatrix} + \begin{bmatrix} \left(\frac{D}{L}\right) \\ 0 \end{bmatrix} \widehat{v_g}(s) + \begin{bmatrix} \left(\left(\frac{V_o}{L}\right) + \left(\frac{V_g}{L}\right)\right) \\ \left(-\frac{V_o}{D'RC}\right) \end{bmatrix} \hat{d}(s) \dots \dots \dots \text{eqn. 4.16}$$

To observe only duty cycle variation effect, keeping  $\widehat{v_g}(s) = 0$ .

$$\Rightarrow s \begin{bmatrix} \hat{i}(s) \\ \hat{v}(s) \end{bmatrix} = \begin{bmatrix} 0 & \left(-\frac{D'}{L}\right) \\ \left(\frac{D'}{C}\right) & \left(-\frac{1}{RC}\right) \end{bmatrix} \begin{bmatrix} \hat{i}(s) \\ \hat{v}(s) \end{bmatrix} + \begin{bmatrix} \left(\left(\frac{V_o}{L}\right) + \left(\frac{V_g}{L}\right)\right) \\ \left(-\frac{V_o}{D'RC}\right) \end{bmatrix} \hat{d}(s)$$

$$\Rightarrow \begin{bmatrix} s & \left(\frac{D'}{L}\right) \\ \left(-\frac{D'}{C}\right) & \left(s + \frac{1}{RC}\right) \end{bmatrix} \begin{bmatrix} \hat{i}(s) \\ \hat{v}(s) \end{bmatrix} = \begin{bmatrix} \left(\left(\frac{V_o}{L}\right) + \left(\frac{V_g}{L}\right)\right) \\ \left(-\frac{V_o}{D'RC}\right) \end{bmatrix} \hat{d}(s)$$

$$\Rightarrow \begin{bmatrix} \hat{i}(s) \\ \hat{v}(s) \end{bmatrix} = \begin{bmatrix} s & \left(\frac{D'}{L}\right) \\ \left(-\frac{D'}{C}\right) & \left(s + \frac{1}{RC}\right) \end{bmatrix}^{-1} \begin{bmatrix} \left(\left(\frac{V_o}{L}\right) + \left(\frac{V_g}{L}\right)\right) \\ \left(-\frac{V_o}{D'RC}\right) \end{bmatrix} \hat{d}(s)$$

$$\Rightarrow \begin{bmatrix} \hat{i}(s) \\ \hat{v}(s) \end{bmatrix} = \left( \frac{1}{\left(s^2 + \frac{s}{RC} + \left(\frac{D'^2}{LC}\right)\right)} \right) \begin{bmatrix} \left(s + \frac{1}{RC}\right) & \left(-\frac{D'}{L}\right) \\ \left(\frac{D'}{C}\right) & s \end{bmatrix} \begin{bmatrix} \left(\left(\frac{V_o}{L}\right) + \left(\frac{V_g}{L}\right)\right) \\ \left(-\frac{V_o}{D'RC}\right) \end{bmatrix} \hat{d}(s)$$

$$\Rightarrow \begin{bmatrix} \hat{i}(s) \\ \hat{v}(s) \end{bmatrix} = \left( \frac{1}{\left(s^2 + \frac{s}{RC} + \left(\frac{D'^2}{LC}\right)\right)} \right) \begin{bmatrix} \left(\frac{V_o + V_g}{L}\right)\left(s + \frac{1}{RC}\right) + \left(-\frac{D'}{L}\right)\left(-\frac{V_o}{D'RC}\right) \\ \left(\frac{V_o + V_g}{L}\right)\left(\frac{D'}{C}\right) + \left(-\frac{sV_o}{D'RC}\right) \end{bmatrix} \hat{d}(s)$$

..... eqn. 4.17

$$\hat{y}(s) = -\hat{v}(s)$$

Hence, from eqn. 4.17,

$$\left(\frac{\hat{y}(s)}{\hat{d}(s)}\right) = - \left[ \frac{\left( \left( \frac{V_o + V_g}{L} \right) \left( \frac{D'}{C} \right) + \left( -\frac{sV_o}{D'RC} \right) \right)}{\left( s^2 + \frac{s}{RC} + \left( \frac{D'^2}{LC} \right) \right)} \right]$$

$$V_o = V_g \left( \frac{D}{D'} \right)$$

$$\Rightarrow (V_g + V_o) = \left( \frac{V_o}{D} \right)$$

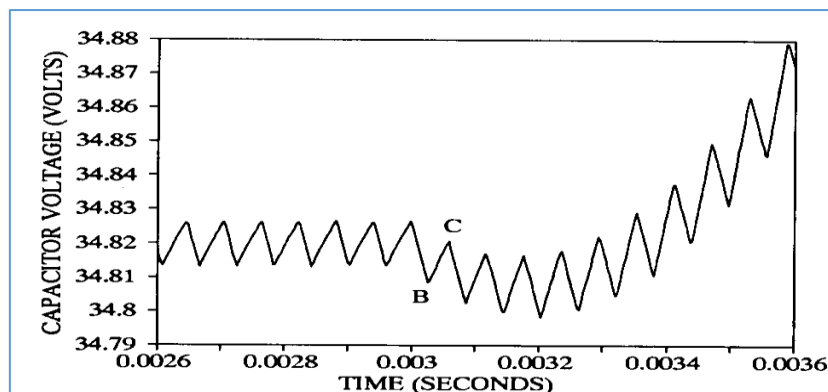
Hence,

$$\left(\frac{\hat{y}(s)}{\hat{d}(s)}\right) = - \left[ \frac{\left( \left( \frac{V_o}{DL} \right) \left( \frac{D'}{C} \right) + \left( -\frac{sV_o}{D'RC} \right) \right)}{\left( s^2 + \frac{s}{RC} + \left( \frac{D'^2}{LC} \right) \right)} \right]$$

$$\Rightarrow \left(\frac{\hat{y}(s)}{\hat{d}(s)}\right) = \left( \frac{V_o}{D'RC} \right) \left[ \frac{\left( \left( -\left( \frac{D'^2 R}{DL} \right) \right) + s \right)}{\left( s^2 + \frac{s}{RC} + \left( \frac{D'^2}{LC} \right) \right)} \right]$$

$$\left(\frac{\hat{y}(s)}{\hat{d}(s)}\right) = \left( \frac{V_o}{D'RC} \right) \left[ \frac{\left( s - \left( \frac{D'^2 R}{DL} \right) \right)}{\left( s^2 + \frac{s}{RC} + \left( \frac{D'^2}{LC} \right) \right)} \right]$$

So from the final transfer function of output voltage variation w.r.t duty ratio variation has a R.H.P zero at  $s = \left( \frac{D'^2 R}{DL} \right)$ . This R.H.P zero creates an undesired voltage drop due to incremental step increase in duty cycle until the recovery of capacitor voltage. This effect of R.H.P zero can be partially minimized by pushing it far from origin of s-plane by decreasing the value of L, increasing the value of R & decreasing the switching frequency or by operating at DCM.



**Capacitor Voltage drop for duty cycle increment, Figure 4.2**

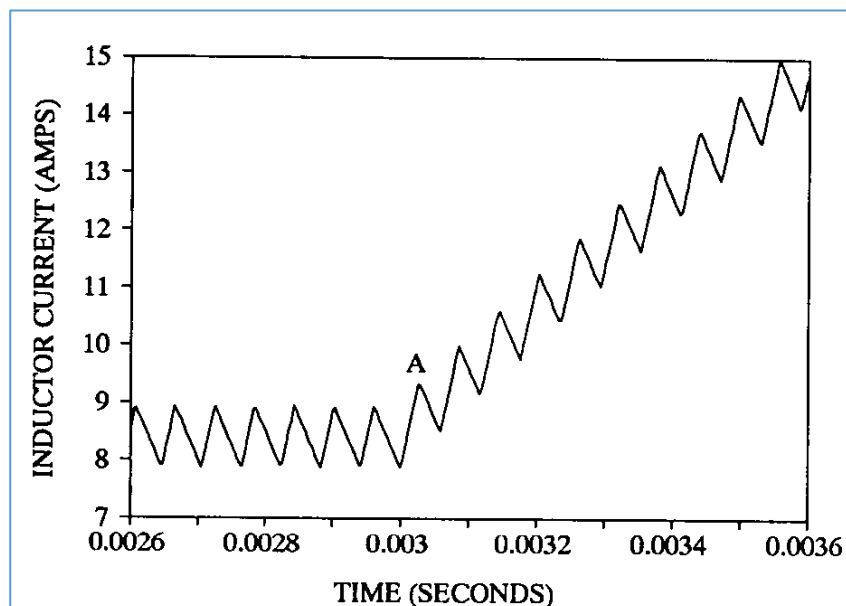
This problem of right half plane zero is prominent at lightly load condition.

Now, from eqn. 4.17,

$$\left(\frac{\hat{i}(s)}{\hat{d}(s)}\right) = \left[ \frac{\left(\frac{V_o+V_g}{L}\right)\left(s + \frac{1}{RC}\right) + \left(-\frac{D'}{L}\right)\left(-\frac{V_o}{D'RC}\right)}{\left(s^2 + \frac{s}{RC} + \left(\frac{D'^2}{LC}\right)\right)} \right]$$

$$\Rightarrow \left(\frac{\hat{i}(s)}{\hat{d}(s)}\right) = \left[ \frac{\left(\frac{V_o}{DL}\right)\left(s + \frac{1}{RC} + \frac{D}{RC}\right)}{\left(s^2 + \frac{s}{RC} + \left(\frac{D'^2}{LC}\right)\right)} \right]$$

Thus there is no R.H.P zero for transfer function of inductor current variation w.r.t duty ratio variation. So due to incremental step change in duty cycle the inductor current increases immediately.



**Immediate Inductor current rise for duty cycle increment, Figure 4.3**

- **First order model analysis of current mode controlled Buck-Boost converter:**

Current mode control removes one pole from  $\left(\frac{\hat{y}(s)}{\hat{d}(s)}\right)$  transfer function. In CCM, if not directly controlling the duty cycle, if inductor current is tracked with a current reference, which in turn indirectly controls the duty cycle.

Thus, in case of current mode control,  $\hat{i}(s) = \hat{i}_c(s)$ ,  $\hat{i}_c(s)$  is reference current signal.

Hence, replacing  $\hat{i}(s)$  by  $\hat{i}_c(s)$ , from eqn. 4.16,

$$s \begin{bmatrix} \hat{i}_c(s) \\ v(s) \end{bmatrix} = \begin{bmatrix} 0 & \left(-\frac{D'}{L}\right) \\ \left(\frac{D'}{C}\right) & \left(-\frac{1}{RC}\right) \end{bmatrix} \begin{bmatrix} \hat{i}_c(s) \\ v(s) \end{bmatrix} + \begin{bmatrix} \left(\frac{D}{L}\right) \\ 0 \end{bmatrix} \widehat{v}g(s) + \begin{bmatrix} \left(\left(\frac{V_o}{L}\right) + \left(\frac{V_g}{L}\right)\right) \\ \left(-\frac{V_o}{D'RC}\right) \end{bmatrix} \hat{d}(s) \dots \text{eqn. 4.18}$$

$$s\hat{i}_c(s) = \left(-\frac{D'}{L}\right)v(s) + \left(\frac{D}{L}\right)\widehat{v}g(s) + \left(\frac{V_o + V_g}{L}\right)\hat{d}(s)$$

$$\hat{d}(s) = \frac{s\hat{i}_c(s) + \left(\frac{D'}{L}\right)v(s) - \left(\frac{D}{L}\right)\widehat{v}g(s)}{\left(\frac{V_o + V_g}{L}\right)}$$

For observing only  $\hat{i}_c(s)$  effect, taking  $\widehat{v}g(s) = 0$ ,

$$\hat{d}(s) = \frac{s\hat{i}_c(s) + \left(\frac{D'}{L}\right)v(s)}{\left(\frac{V_o + V_g}{L}\right)}$$

Again from eqn. 4.18, we get,

$$sv(s) = v(s)\hat{i}_c(s) + \left(-\frac{1}{RC}\right)v(s) + \left(-\frac{V_o}{D'RC}\right)\hat{d}(s)$$

Putting the value of  $\hat{d}(s)$ , and  $(V_g + V_o) = \left(\frac{V_o}{D}\right)$

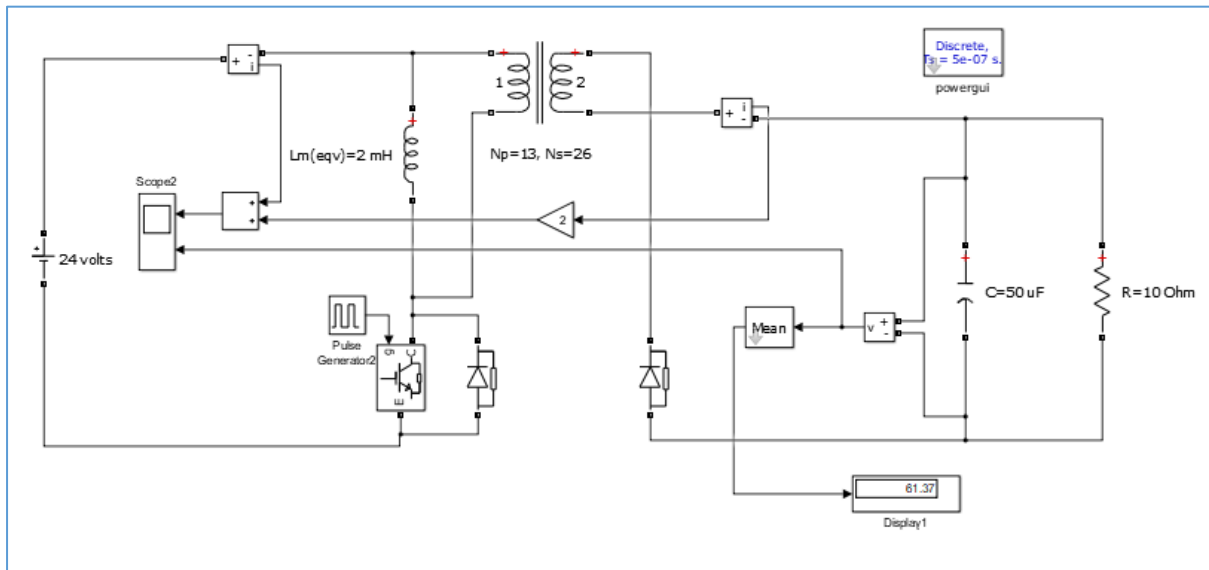
$$sv(s) = v(s)\hat{i}_c(s) + \left(-\frac{1}{RC}\right)v(s) + \left(-\frac{V_o}{D'RC}\right)\frac{s\hat{i}_c(s) + \left(\frac{D'}{L}\right)v(s)}{\left(\frac{V_o}{DL}\right)}$$

After some manipulation,

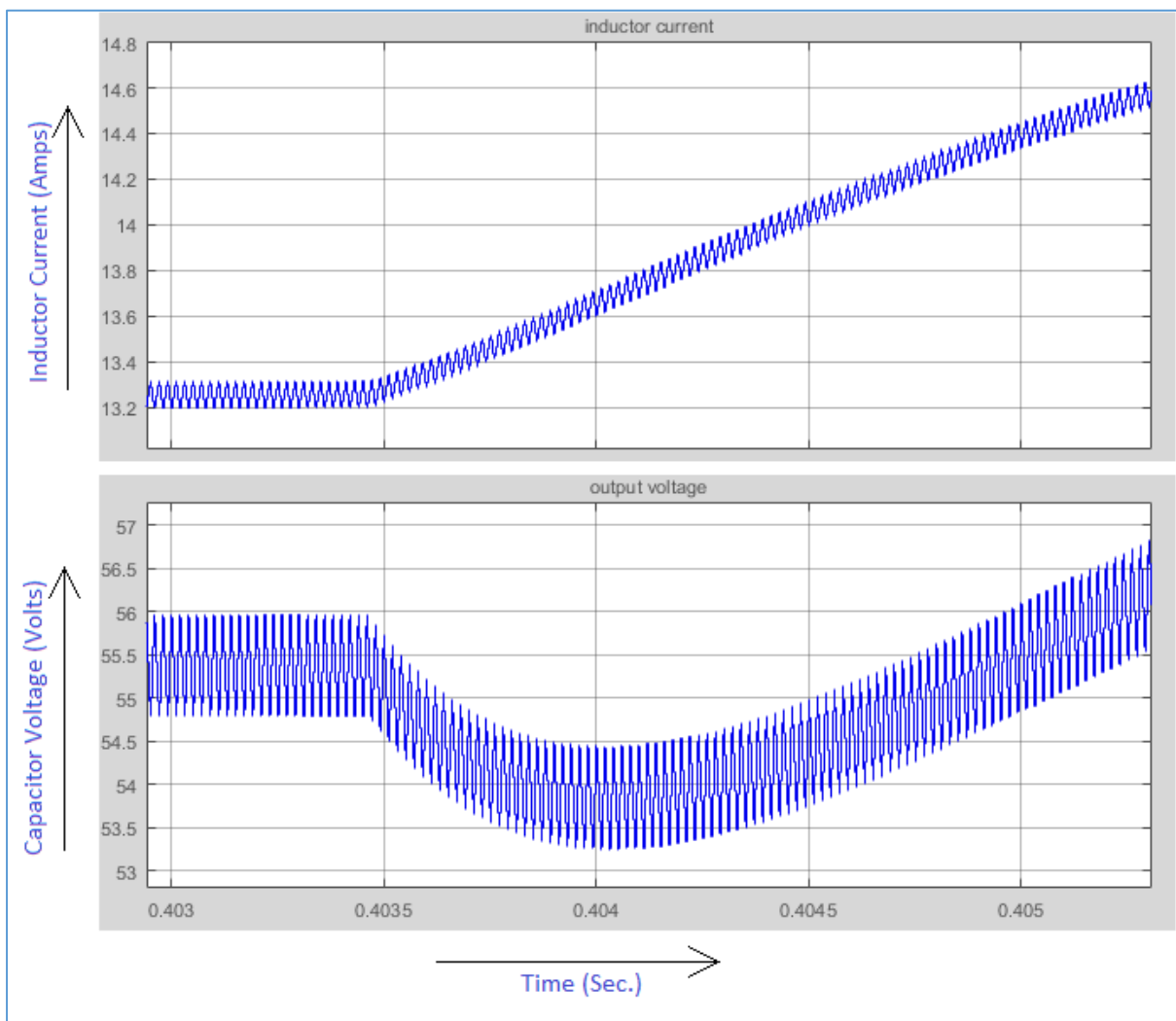
$$\begin{aligned} \left(\frac{v(s)}{\hat{i}_c(s)}\right) &= \frac{D'RC}{1+D} \frac{\left(1 - \frac{sDL}{D'^2R}\right)}{\left(1 + \frac{sRC}{1+D}\right)} \\ \Rightarrow \left(\frac{\hat{y}(s)}{\hat{i}_c(s)}\right) &= -\frac{D'RC}{1+D} \frac{\left(1 - \frac{sDL}{D'^2R}\right)}{\left(1 + \frac{sRC}{1+D}\right)} \end{aligned}$$

Hence, current mode control removes one pole from the control-to-output transfer function, thus simplifying the compensation in negative-feedback system, especially in the presence of the right-half-plane zero.

• **Matlab simulation study of RHP zero effect at CCM:**



**Simulink model of Flyback converter with resistive load, Figure 4.4**



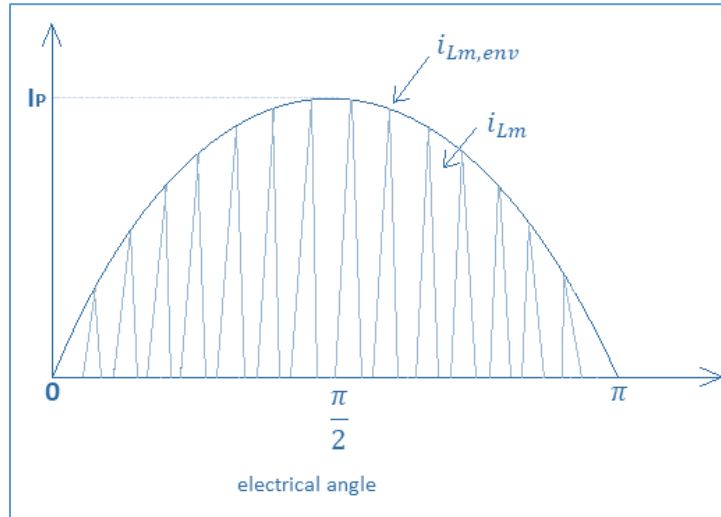
**Simulated waveform of inductor current and output voltage of Flyback converter due to incremental step change in duty cycle from  $d=0.55$  to  $d=0.552$ , Figure 4.5**



## CHAPTER- 5

### Single-stage inverter operation at DCM

- **Calculation of 'Lm' for DCM operation:**



**Inductor current at DCM during half cycle of utility grid line, Figure 5.1**

Converter is to be designed to operate magnetizing inductance in DCM. So sufficient off time must be provided to decrease the  $i_{Lm}$  to zero in each switching cycle. The worst case occurs at the crest point of  $i_{Lm}$ , when the converter operates at maximum duty cycle. At the crest point  $i_{Lm,env}$  is 'Ip'. So at crest point  $(t_{ON} + t_{OFF})$  is just equal to  $(1/2Nf)$  at boundary condition. Where,  $f$  is utility grid frequency,  $N$  is number of switching cycles during half cycle  $(1/2f)$ . So, at crest point,

$$t_{ON} = L_m \frac{I_p}{v_{in}}$$

$$t_{OFF} = L_m \frac{I_p}{N_{tr} V_{grid\_peak}}, \quad \text{Where, } N_{tr} = \left( \frac{N_p}{N_s} \right).$$

Hence,

$$t_{ON} + t_{OFF} \leq (1/2Nf)$$

$$L_m \frac{I_p}{v_{in}} + L_m \frac{I_p}{N_{tr} V_{grid\_peak}} \leq (1/2Nf)$$

$$L_m I_p \left( \frac{1}{v_{in}} + \frac{1}{N_{tr} V_{grid\_peak}} \right) \leq (1/2Nf)$$

$$L_m \leq \frac{v_{in} N_{tr} V_{grid\_peak}}{2Nf I_p (v_{in} + N_{tr} V_{grid\_peak})} \dots \dots \dots \text{eqn. 5.1}$$

- **Matlab simulation study of Single-stage inverter (At DCM):**

Here for simulation we have taken  $v_{in} = 100 \text{ Volts}$ ,  $V_{grid\_peak} = 100 \text{ Volts}$ ,  $N_{tr} = \left(\frac{13}{20}\right)$ ,

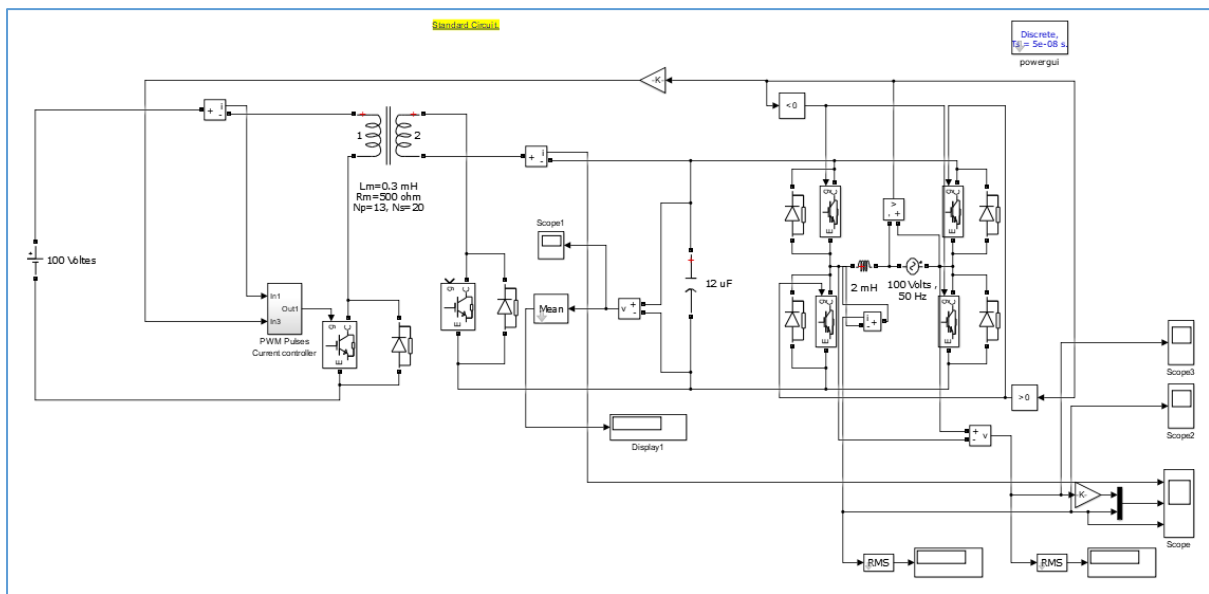
$$f = 50 \text{ Hz}, f_{sw} = 6 \text{ kHz}, I_p = 20. \text{ So, } N = \left(\frac{f_{sw}}{2f}\right) = \left(\frac{6k}{2 \times 50}\right).$$

Hence, from eqn. 5.1,

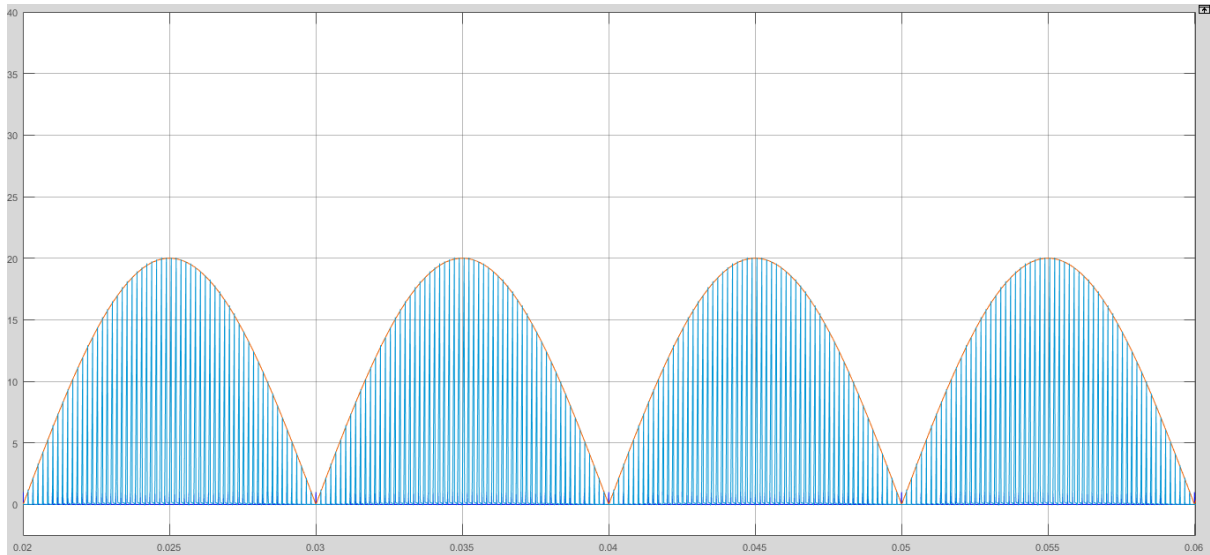
$$L_m \leq \frac{100 \times \left(\frac{13}{20}\right) \times 100}{2 \times \left(\frac{6k}{2 \times 50}\right) \times 50 \times 20 \times \left(100 + \left(\frac{13}{20}\right) \times 100\right)}$$

$$L_m \leq 0.32828 \text{ mH}$$

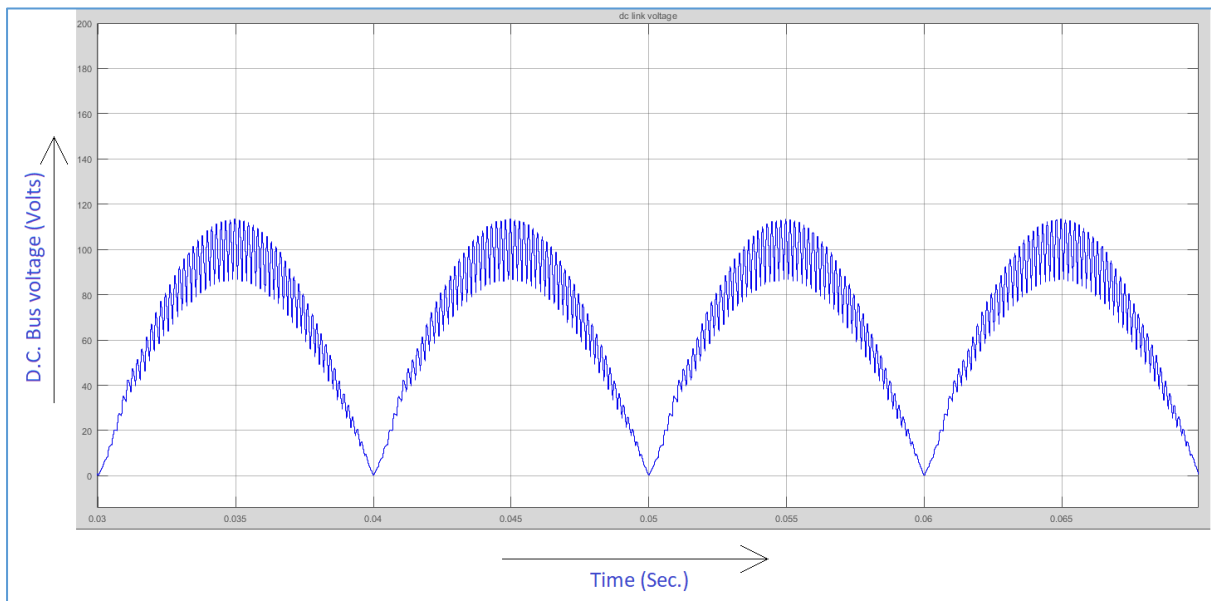
So for DCM we have taken  $L_m = 0.3 \text{ mH}$ .



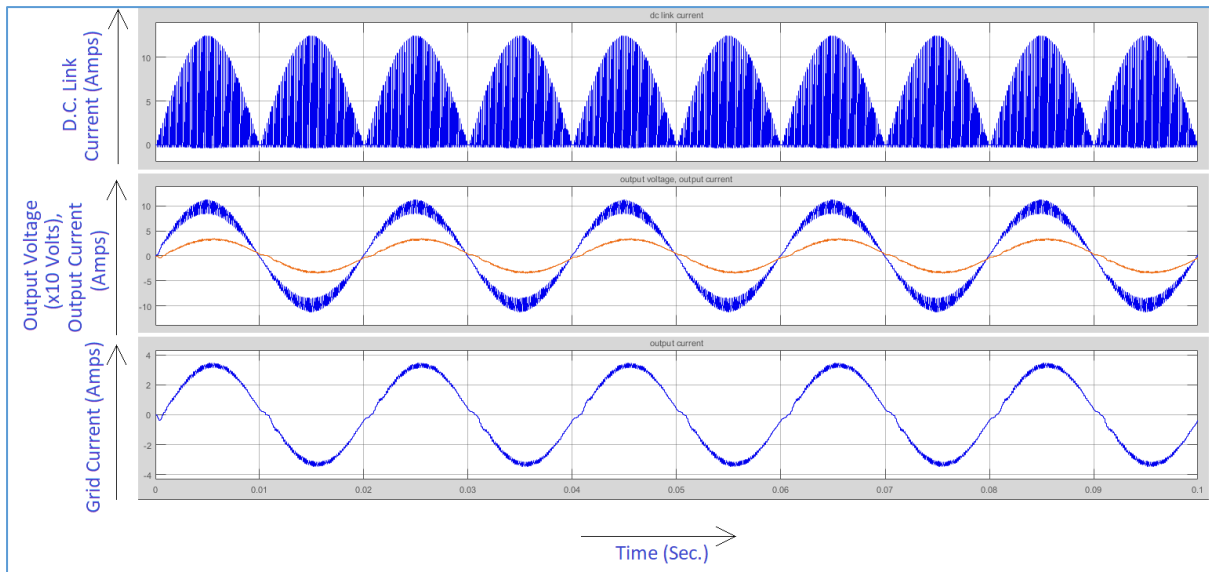
**Grid connected Single-stage inverter (Discharging mode) , Figure 5.2**



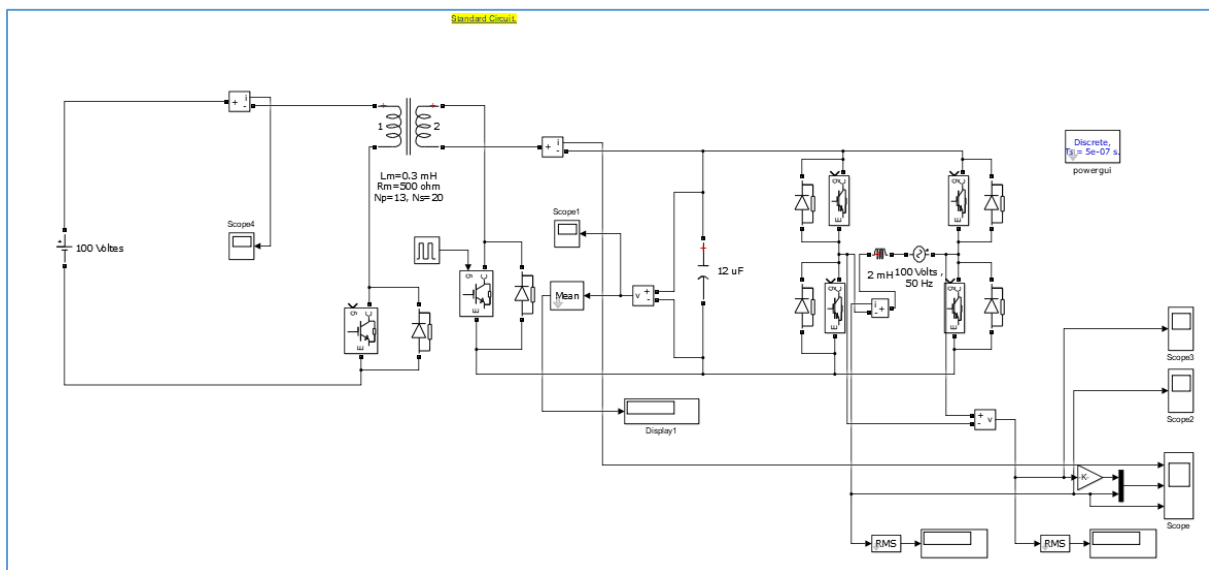
**Switch current waveform for  $f_{sw}=6$  kHz (At DCM) , Figure 5.3**



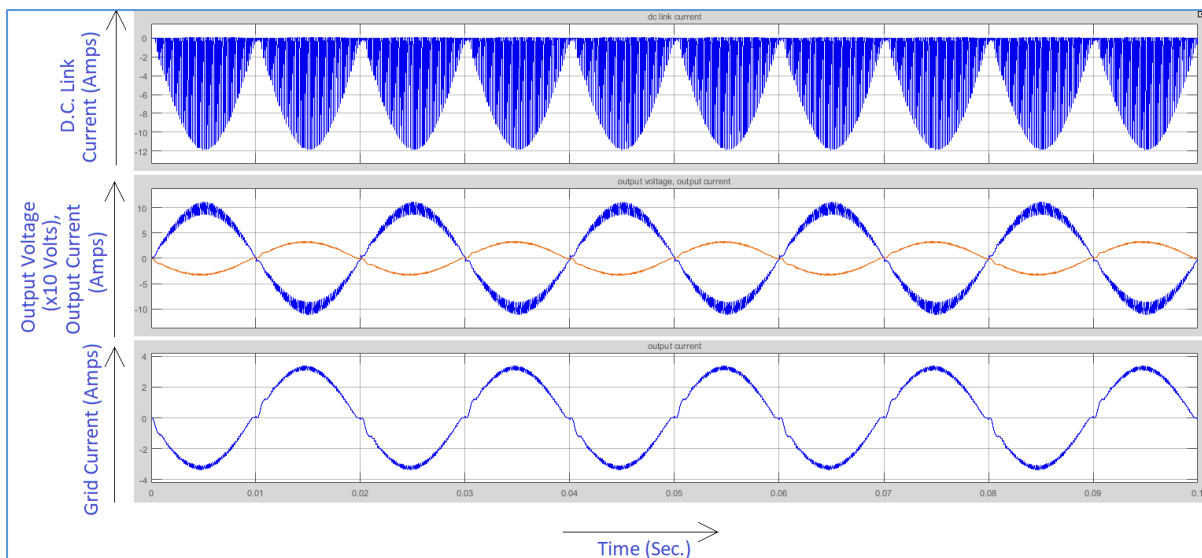
**Dc bus voltage waveform, Figure 5.4**



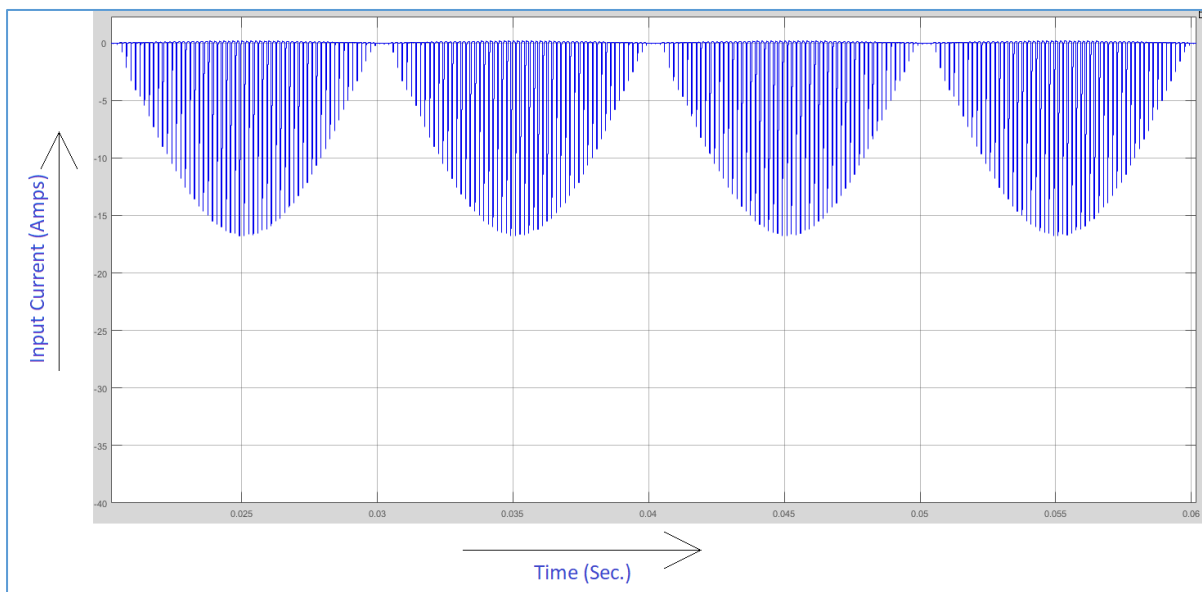
**Simulated waveform of a) dc link current, b) output voltage(X10) & output current, c) grid current at discharging mode, Figure 5.5**



**Single-stage inverter at charging mode with  $f_{inv}=6$  kHz, duty cycle=50%, Figure 5.6**



**Simulated waveform of a) dc link current, b) output voltage(X10) & output current, c) grid current at charging mode of Single-stage inverter, Figure 5.7**

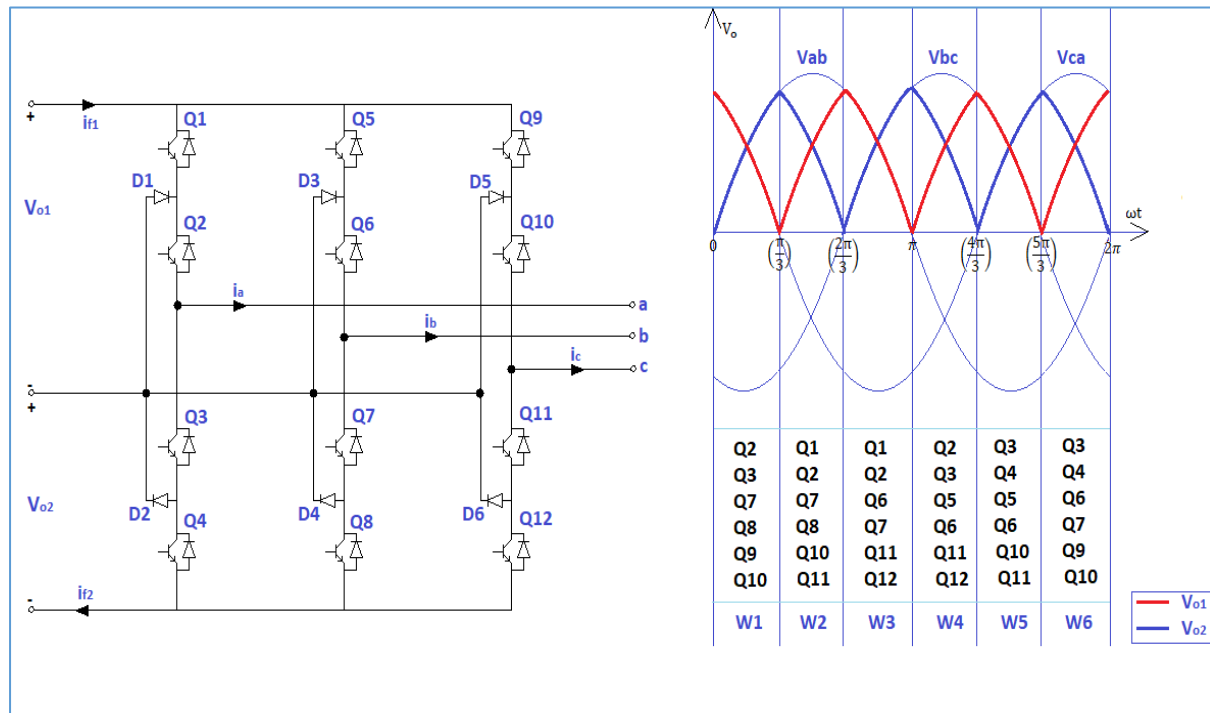


**Input dc current waveform of Single-stage inverter at charging mode, Figure 5.8**

## CHAPTER- 6

### Single-stage inverter operation extended to three-phase.

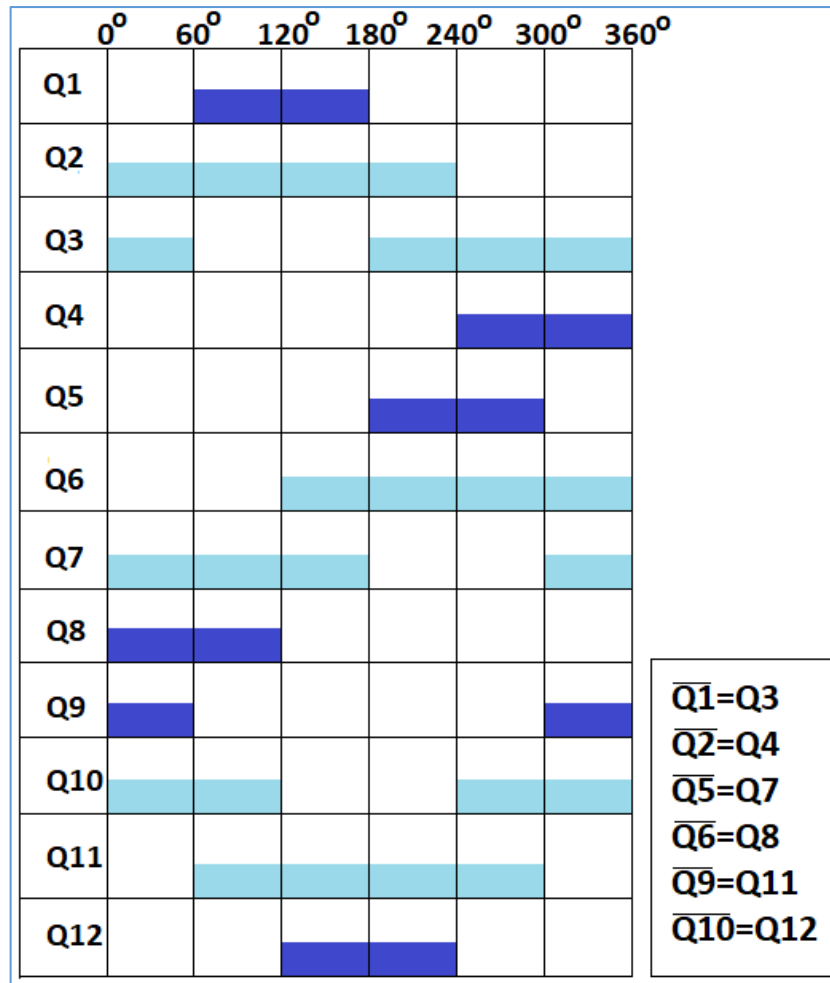
- Description of three phase unfolder bridge operation with single stage Flyback converter.



**Three phase Unfolder Bridge with graphical representation of its operation, Figure 6.1**

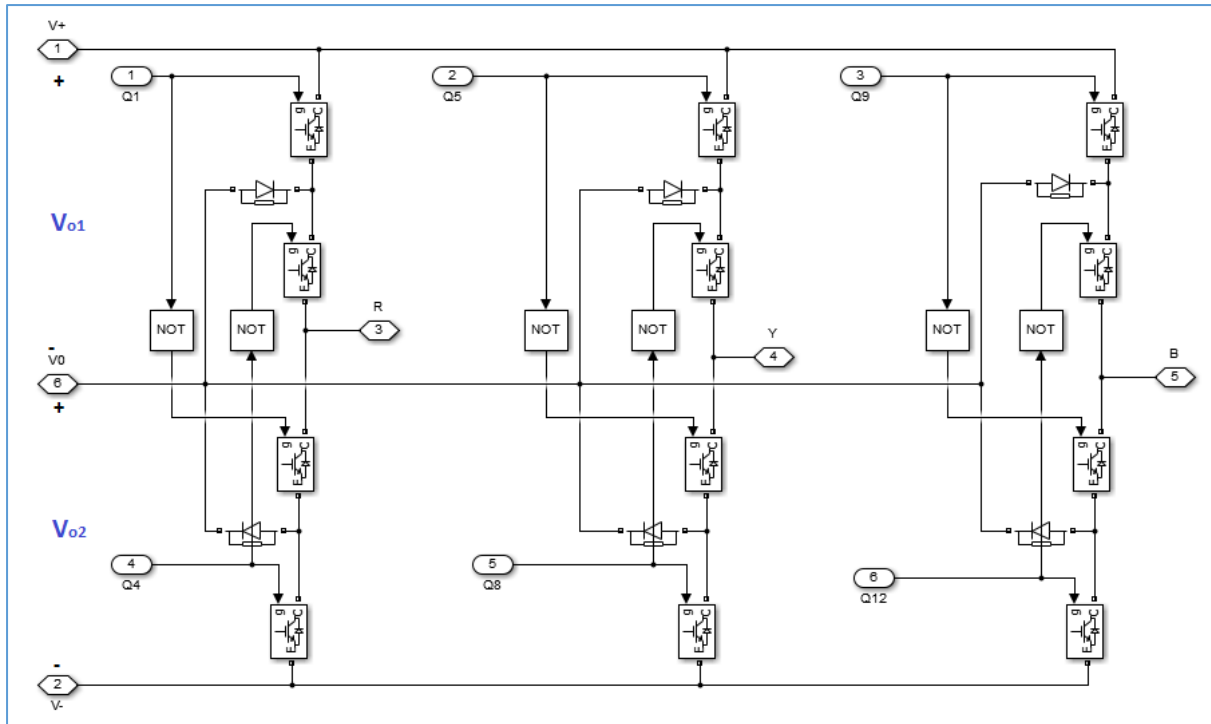
Two Flyback converter output currents are modulated as required dc link currents to produce the desired sinusoidal ac line currents. Switching sequence of three phase Unfolder Bridge is arranged in such a manner that the time varying current of Flyback converters is reconstructed into sinusoidal ac currents by the unfolder. In grid-tied configuration, the supplied ac voltages are rectified into time-varying positive voltages in the dc-link. By generating dc-link currents with the appropriate time-varying wave profile using two Flyback converter, the desired ac currents are obtained.

The unfolder is controlled using a state variable 'w'. For every multiple of 60 degree in theta, 'w' updates once. This produces a sequence containing six states, in each of which a different set of unfolder switches are activated. This switching action produces a pair of time varying voltages  $V_{o1}$  and  $V_{o2}$  in the dc-link as shown in the figure. The dc-link voltages overlap with portions of the line-line voltages.



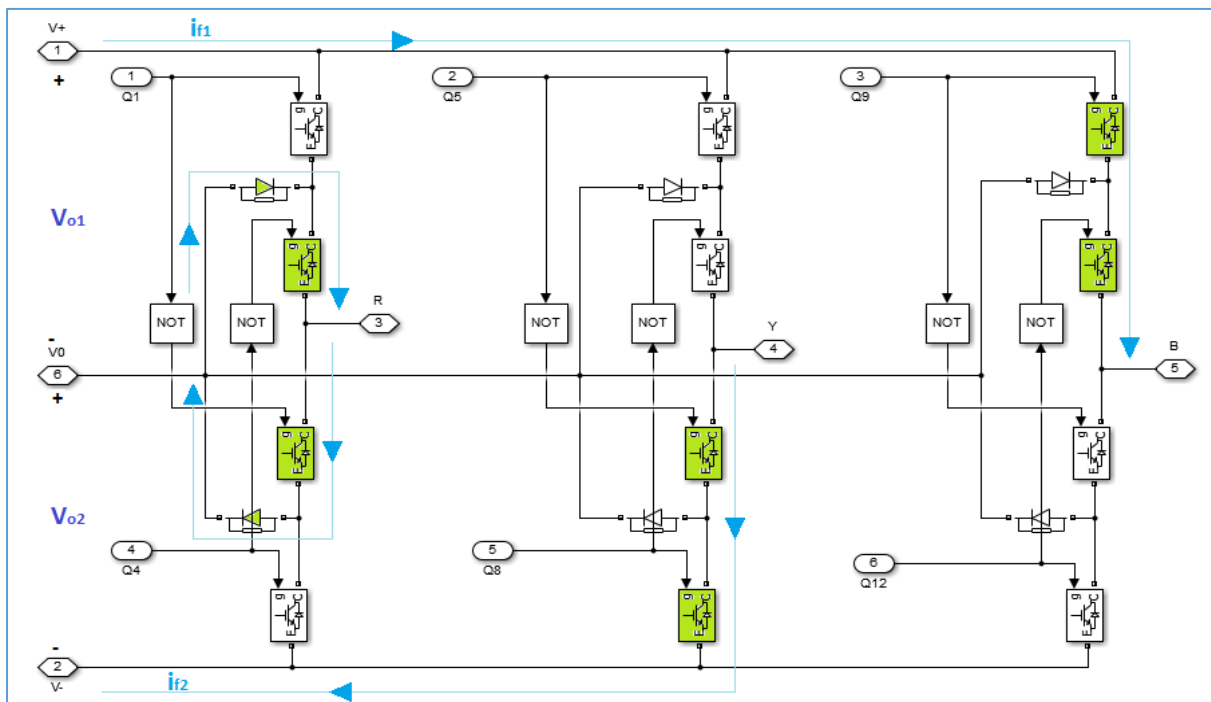
**Pulse Sequence & pulse relation of switches of three phase Unfolder Bridge , Figure 6.2**

So, from pulse sequence table and pulse relations, by creating pulses of Q1, Q4, Q5, Q8, Q9, Q12 and by applying inverted pulses of them on remaining switches as per the relation, we can operate the three phase Unfolder Bridge.



**Matlab model of three phase Unfolder Bridge, Figure 6.3**

### Window 1 operation:

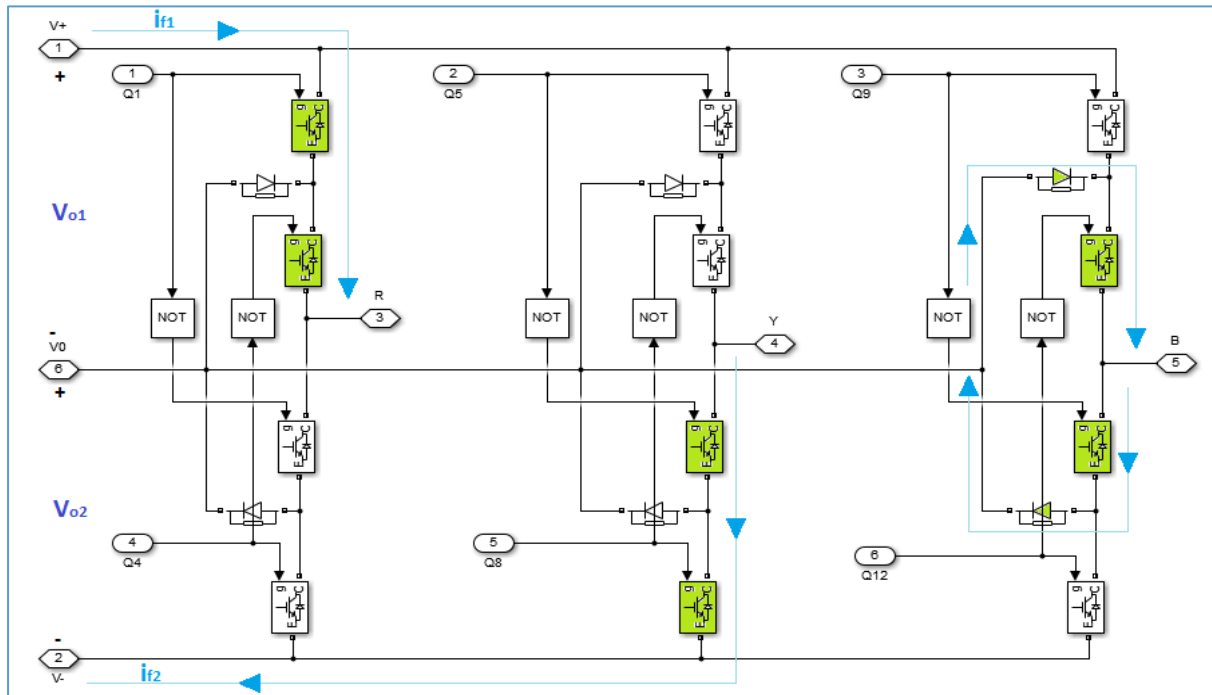


**Unfolding bridge operation at window 1, Figure 6.4**

During window 1 operation Q2, Q3, Q7, Q8, Q9, and Q10 is on and through two antiparallel diodes as shown in the figure, bridge current flows through the three phase grid. Hence, from figure  $i_{f1}=i_B$  and  $i_{f2}=-i_Y$  and grid voltages appears across two dc buses through line inductance as  $V_{o1}=V_{BR}$  and  $V_{o2}=V_{RY}$  which is synchronised with two Flyback converter output voltages.



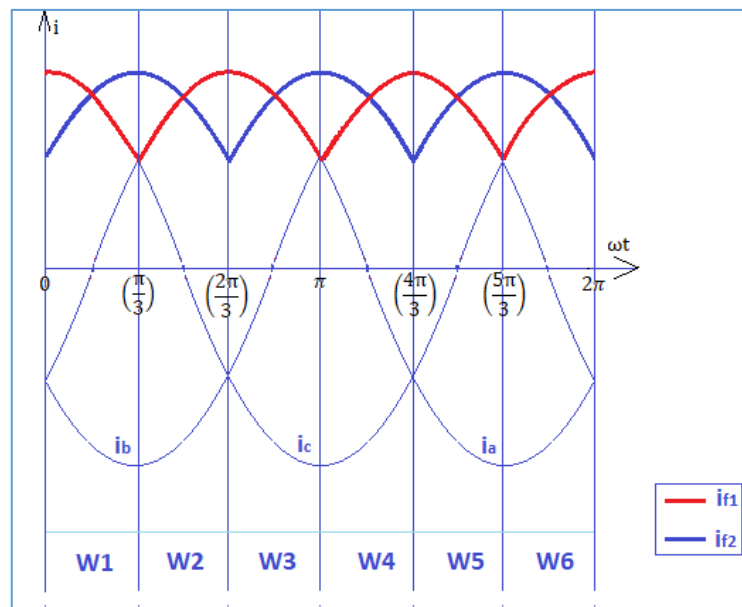
## Window 2 operation:



**Unfolding bridge operation at window 2, Figure 6.5**

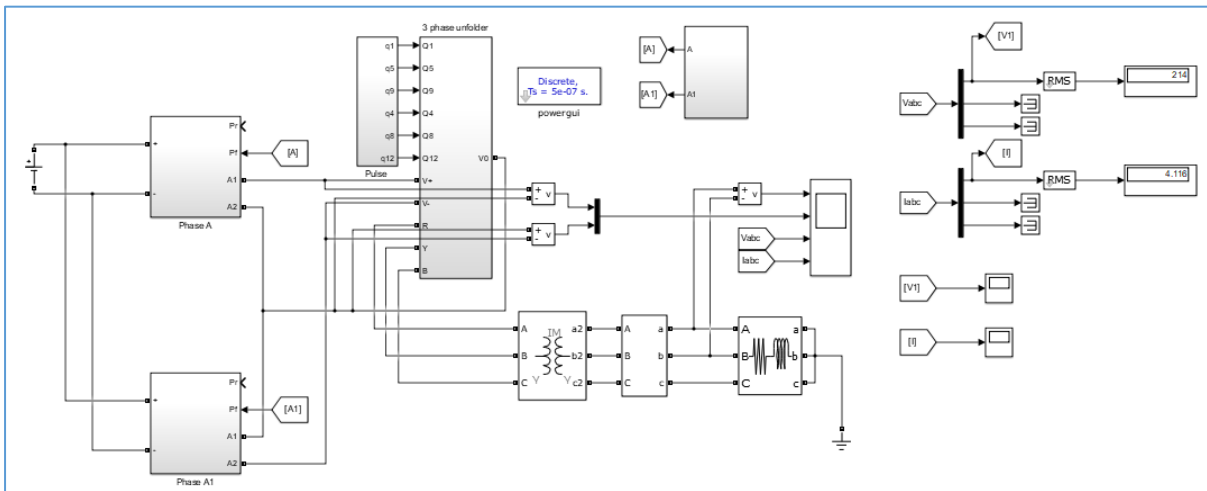
Similarly during window 2 operation Q1, Q2, Q7, Q8, Q10 and Q11 is on and through the shown antiparallel diodes bridge current flows,  $i_{f1}=i_R$  and  $i_{f2}=-i_Y$  and thus  $V_{o1}=V_{RB}$  and  $V_{o2}=V_{BY}$ .

In this way all the six windows continues periodically and Flyback converter with three phase unfolder, feeds power to the grid synchronously.



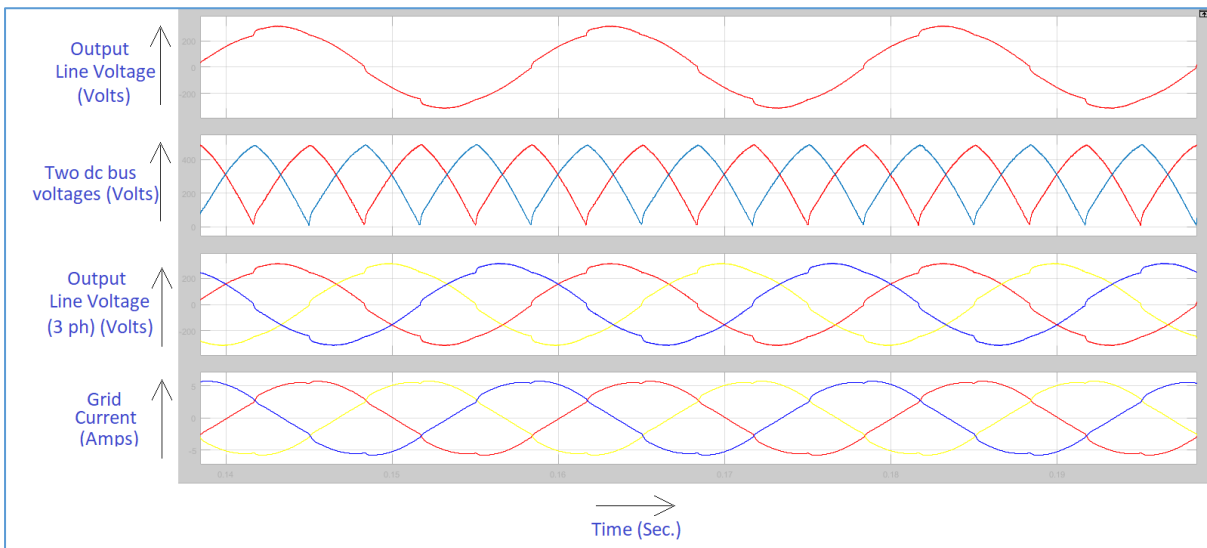
**dc link currents( $i_{f1}$  &  $i_{f2}$ ) and reconstructed ac currents( $i_a$ ,  $i_b$  &  $i_c$ ), Figure 6.6**

• Matlab simulation study of single stage three phase system.

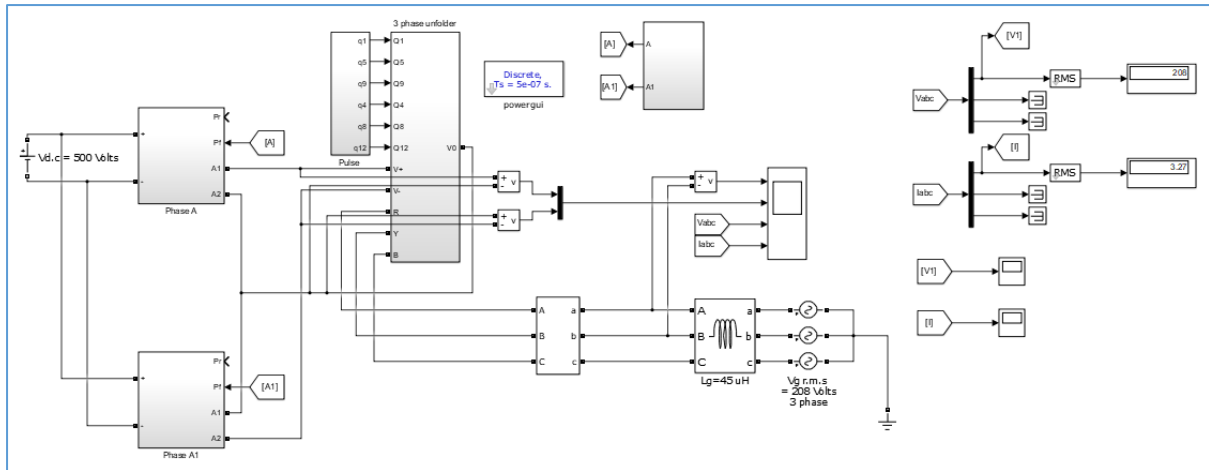


**Flyback converter with three phase unfollder with three phase star connected R-L load,**

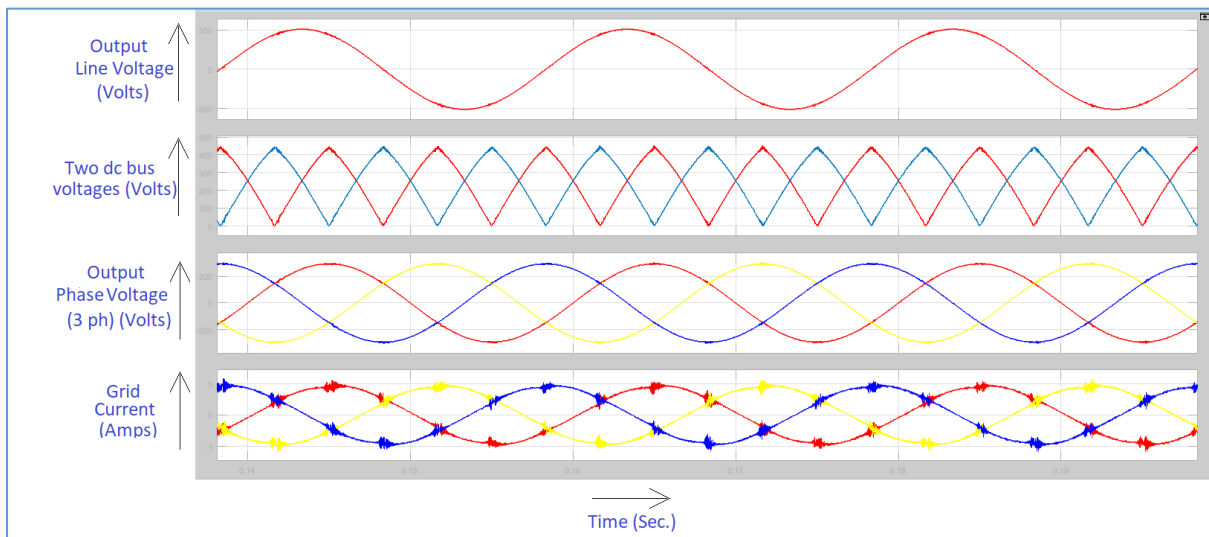
**Figure 6.7**



**a) Output Line voltage, b) 90 degree phase shifted two dc bus voltages (f=150 Hz), c) Output line voltage (three phase), d) Output load current (three phase) , Figure 6.8**



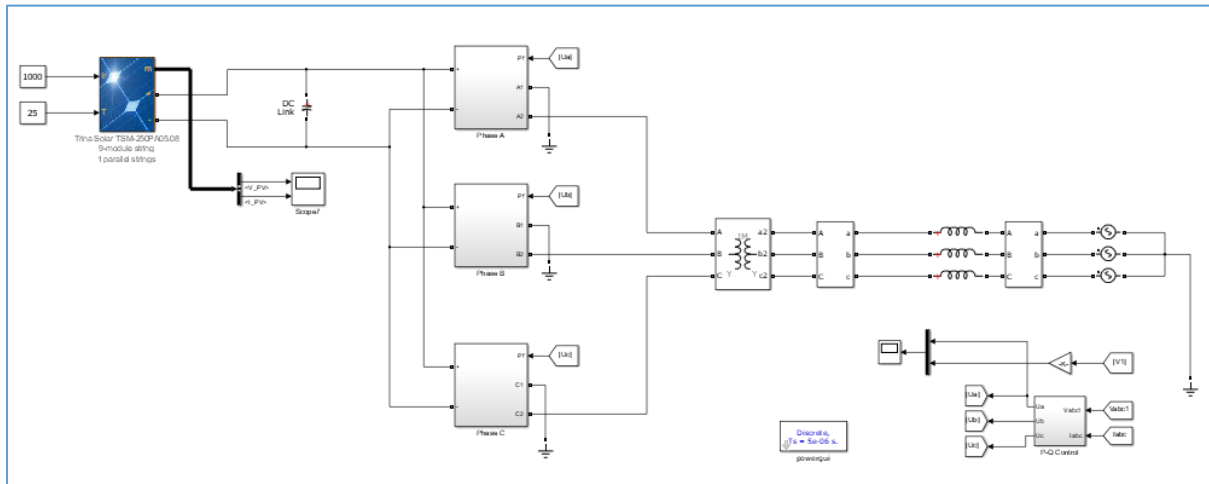
**Flyback converter with three phase unfolded (Grid connected, without transformer) ,**  
**Figure 6.9**



**a) Output Line voltage, b) 90 degree phase shifted two dc bus voltages (f=150 Hz), c)**  
**Output phase voltage (three phase), d) Output load current (three phase) , Figure 6.10**

# CHAPTER-7

## Study of three phase scheme of single stage conversion.

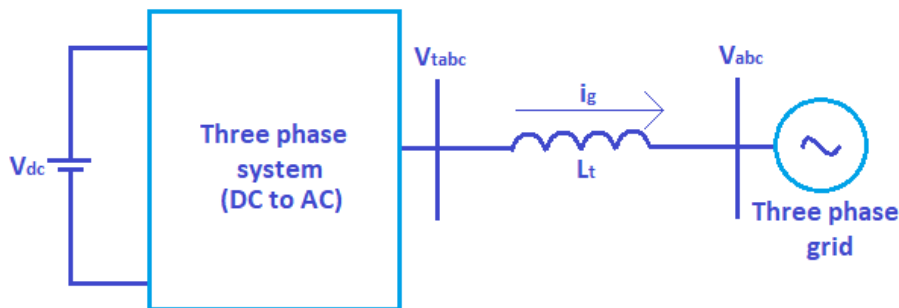


**Matlab model of three phase scheme, Figure 7.1**

In the proposed three phase scheme, three Flyback inverter output is 120 degree out of phase from each other. Output of these three Flyback inverter is fed to the grid through a three phase 1200 by 600 Y-Y power transformer and line inductance  $L_g = 0.5$  mH. Input is a PV panel and peak value of grid voltage is 100 volts.

Sinusoidal Current reference for three Flyback inverter is generated from three phase grid through d-q control loop and current of the inductor is tracked using a hysteresis band current controller.

- **D-Q control theory:**



$$[V_{tabc}] = [L_t] \left( \frac{d[i_g]}{dt} \right) + [V_{abc}]$$

$$\begin{bmatrix} V_{ta} \\ V_{tb} \\ V_{tc} \end{bmatrix} = \begin{bmatrix} L_{ta} & 0 & 0 \\ 0 & L_{tb} & 0 \\ 0 & 0 & L_{tc} \end{bmatrix} \begin{bmatrix} \dot{i}_a \\ \dot{i}_b \\ \dot{i}_c \end{bmatrix} + \begin{bmatrix} V_a \\ V_b \\ V_c \end{bmatrix} \dots \dots \dots \text{eqn. 7.1}$$

$$L_{ta} = L_{tb} = L_{tc} = L$$

**abc frame to  $\alpha - \beta$  frame transformation:**

$$\begin{bmatrix} r_\alpha \\ r_\beta \end{bmatrix} = \begin{bmatrix} 1 & -\frac{1}{2} & -\frac{1}{2} \\ 0 & \frac{\sqrt{3}}{2} & -\frac{\sqrt{3}}{2} \end{bmatrix} \begin{bmatrix} r_a \\ r_b \\ r_c \end{bmatrix} = [C] \begin{bmatrix} r_a \\ r_b \\ r_c \end{bmatrix}$$

Hence, from eqn. 7.1,

$$[V_{tabc}] = [L_t] \left( \frac{d[i_g]}{dt} \right) + [V_{abc}]$$

$$[C]^{-1}[V_{t\alpha\beta}] = [L_t][C]^{-1} \left( \frac{d[i_{\alpha\beta}]}{dt} \right) + [C]^{-1}[V_{\alpha\beta}]$$

$$[V_{t\alpha\beta}] = [C][L_t][C]^{-1} \left( \frac{d[i_{\alpha\beta}]}{dt} \right) + [V_{\alpha\beta}]$$

$$\begin{bmatrix} V_{t\alpha} \\ V_{t\beta} \end{bmatrix} = \begin{bmatrix} L & 0 \\ 0 & L \end{bmatrix} \begin{bmatrix} \dot{i}_\alpha \\ \dot{i}_\beta \end{bmatrix} + \begin{bmatrix} V_\alpha \\ V_\beta \end{bmatrix} \dots \dots \dots \text{eqn. 7.2}$$

 **$\alpha - \beta$  frame to d-q frame transformation:**

$$R_{dq} = e^{-j\omega t} R_{\alpha\beta}$$

$$R_{\alpha\beta} = e^{j\omega t} R_{dq}$$

Hence, from eqn. 7.2, in complex form,

$$(V_{t\alpha} + jV_{t\beta}) = L \left( \frac{d(i_\alpha + ji_\beta)}{dt} \right) + (V_\alpha + jV_\beta)$$

$$e^{j\omega t}(V_{td} + jV_{tq}) = L \left( \frac{d(e^{j\omega t}(i_d + ji_q))}{dt} \right) + e^{j\omega t}(V_d + jV_q)$$

$$(V_{td} + jV_{tq}) = e^{-j\omega t} L \left( \frac{d(e^{j\omega t}(i_d + ji_q))}{dt} \right) + (V_d + jV_q)$$

$$(V_{td} + jV_{tq}) = e^{-j\omega t} L \left( j\omega e^{j\omega t}(i_d + ji_q) + e^{j\omega t} \left( \frac{d(i_d + ji_q)}{dt} \right) \right) + (V_d + jV_q)$$

$$(V_{td} + jV_{tq}) = L \left( j\omega(i_d + ji_q) + \left( \frac{d(i_d + ji_q)}{dt} \right) \right) + (V_d + jV_q)$$

$$V_{td} = -\omega L i_q + L \frac{di_d}{dt} + V_d \dots \dots \dots \text{eqn. 7.3.1}$$

$$V_{tq} = \omega L i_d + L \frac{di_q}{dt} + V_q \dots \dots \dots \text{eqn. 7.3.2}$$

Thus the KVL in abc frame is transformed into d-q frame where all terms are dc quantities.

So, at steady state  $\frac{di_d}{dt} = 0$  and  $\frac{di_q}{dt} = 0$ .

Hence from eqn. 7.3.1 & eqn. 7.3.1, at steady state the KVL in d-q frame is,

$$V_{td} = -\omega L i_q + V_d$$

$$V_{tq} = \omega L i_d + V_q$$

These equations are very useful for close loop control purpose as all terms are constant (dc). So, we can use set point controller i.e. simple PID controller. Here we have used only I=1000 in place of PID. Thus from this d-q frame equation we can get d-q voltage of DC to AC converter three phase output voltage.

#### d-q frame to $\alpha - \beta$ frame transformation:

$$R_{\alpha\beta} = e^{j\omega t} R_{dq}$$

$$\begin{bmatrix} r_\alpha \\ r_\beta \end{bmatrix} = \begin{bmatrix} \cos\omega t & -\sin\omega t \\ \sin\omega t & \cos\omega t \end{bmatrix} \begin{bmatrix} r_d \\ r_q \end{bmatrix}$$

#### $\alpha - \beta$ frame to abc frame transformation:

$$\begin{bmatrix} r_a \\ r_b \\ r_c \end{bmatrix} = \begin{bmatrix} \frac{2}{3} & 0 \\ -\frac{1}{3} & \frac{1}{\sqrt{3}} \\ -\frac{1}{3} & -\frac{1}{\sqrt{3}} \end{bmatrix} \begin{bmatrix} r_\alpha \\ r_\beta \end{bmatrix}$$

Thus by using above two transformations on d-q frame equations and dividing them by peak voltage of grid we can get  $U_a, U_b, U_c$  which is used to generate rectified sinusoid current reference for three individual Flyback converters respectively.

- P-Q control:

$$S = \left(\frac{3}{2}\right) V_{dq} I_{dq}^*$$

$$S^* = \left(\frac{3}{2}\right) V_{dq}^* I_{dq}$$

$$(P - iQ) = \left(\frac{3}{2}\right) (V_d - jV_q)(I_d + jI_q)$$

$$P = \left(\frac{3}{2}\right) (V_d I_d + V_q I_q) \dots \dots \dots \text{eqn. 7.4.1}$$

$$Q = \left(\frac{3}{2}\right) (V_d I_q - V_q I_d) \dots \dots \dots \text{eqn. 7.4.2}$$

It is possible to make  $V_q = 0$ , when the rotating frame alignment at  $\omega t = 0$  is 90 degrees behind phase 'a' axis, a positive-sequence signal with Mag=1 & Phase=0 degrees yields the following d-q values: d=1, q=0.

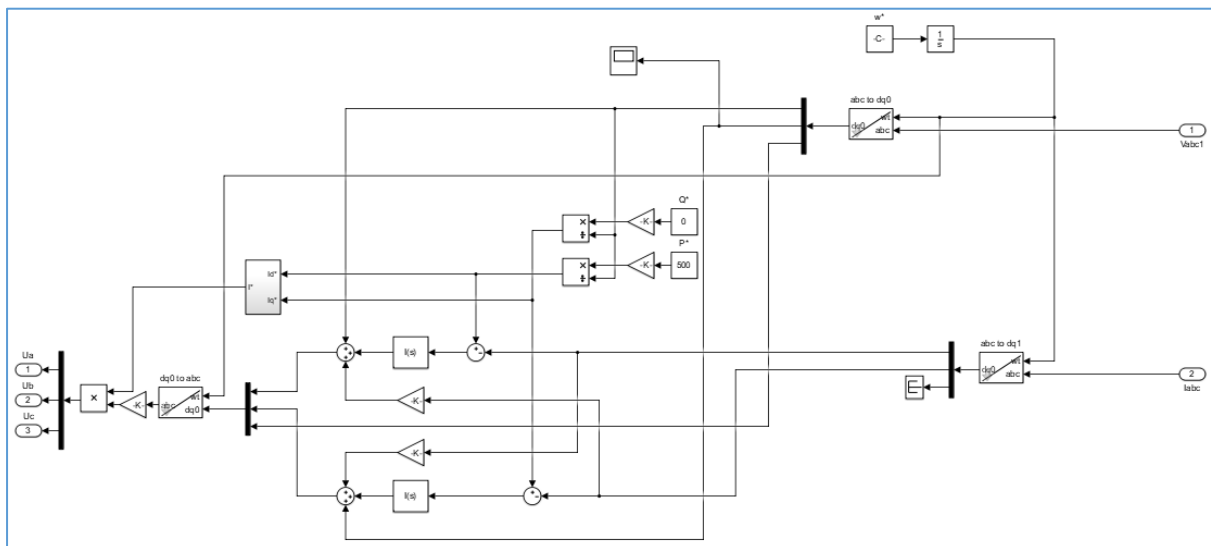
Hence, from eqn. 7.4.1 & eqn. 7.4.2,

$$I_{dref} = \left(\frac{2}{3}\right) \left(\frac{P}{V_d}\right) \text{ and } I_{qref} = \left(\frac{2}{3}\right) \left(\frac{Q}{V_d}\right)$$

$(I_{dref} - I_d)$  &  $(I_{qref} - I_q)$  is fed through PI controller and added with the d-q axis KVL equation. In this way we can control the output voltage to get desired P and Q value. Here in the system P value is controlled by controlling the value of current reference.

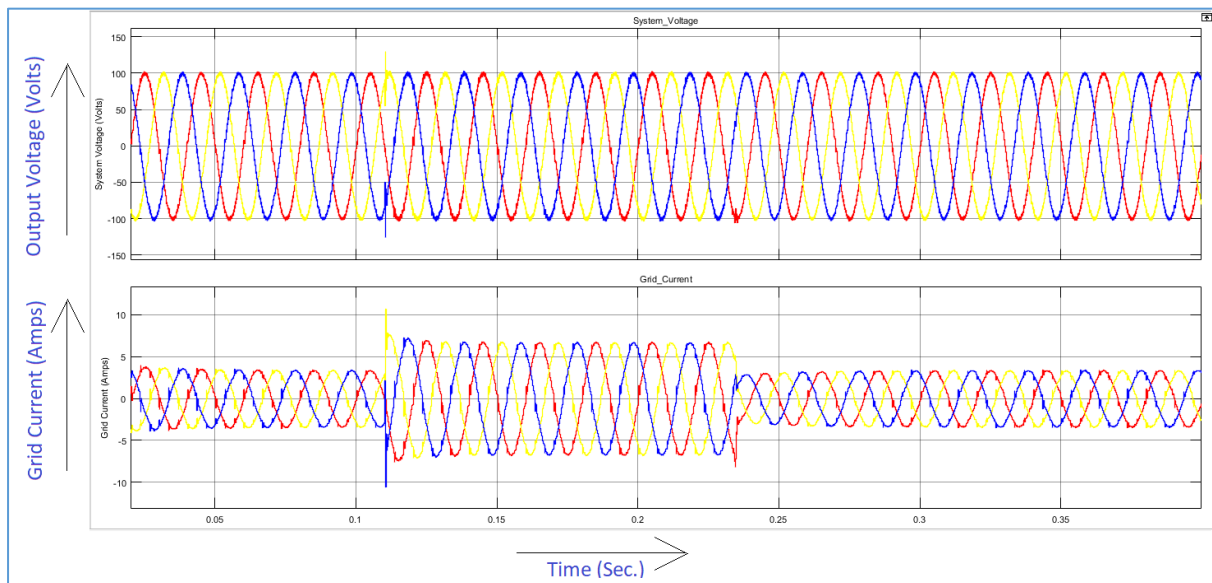
$$I^* = \sqrt{I_{dref}^2 + I_{qref}^2}$$

By varying current reference value of the converter proportionately with  $I^*$  value we can vary the amount of current drawn by the converter in a short range.

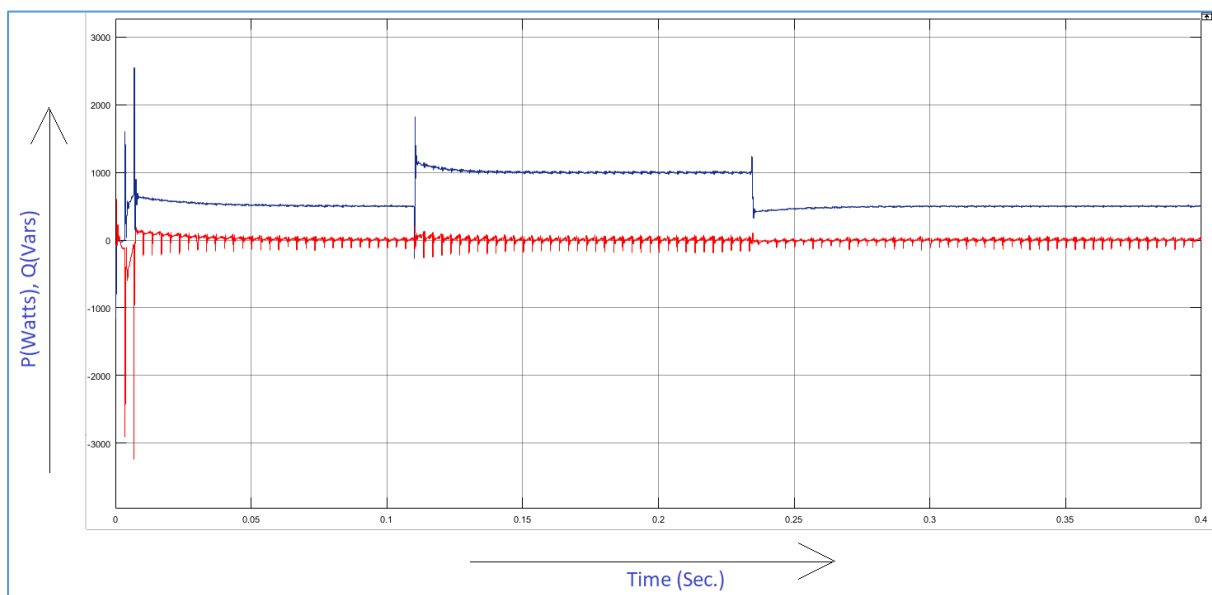


**P-Q control block, Figure 7.2**

- **Matlab simulation study of three phase scheme.**



**Output voltage and grid current waveform, Figure 7.3**



**P-Q curve, Figure 7.4**

So, by setting  $P=500$  and  $Q=0$  we are getting output power as 500 watts and  $Q=0$  Vars. Changing the  $P$  value to 1000 and again returning to 500 we are getting output power at steady state accordingly as per the reference  $P$ .



## CHAPTER- 8

### Discussion and conclusion:

Single-stage inverter is suitable for low power application. It is different from conventional dc to ac converters which uses a separate dc/dc converter to stabilize PV cell output voltage, step up/step down operation before conventional inverter as those inverters are step down inverters. Thus due to two stage operation is less efficient for power transfer from non-conventional energy sources to utility grid. On the other hand Single-stage inverter is more compact and attractive can modulate the power full filling necessary requirement i.e. it step up/step-down and inversion in single stage. Single-stage inverters are derived from dc/dc converters. Among them DAB driven and Flyback converter topology driven single-stage conversions are more popular, as those two converters provide transformer isolation between i/p and o/p and due to high frequency operation, the transformer size reduces drastically which makes the system more compact and efficient. DAB converter can provide bidirectional power flow. As DAB has only step down property, to match output voltage with the grid voltage we have to use high turns ratio transformer. But Flyback converter has both step-up and step down property it does not require high turns ratio to match with grid voltage. Thus in this thesis we have concentrated on Flyback converter driven single-stage conversion. Flyback converter can be operated in both CCM and DCM. DCM is preferable for its better performance to generate smooth sinusoidal grid current, though DCM gives more current spikes which gives stress on switches, is not in CCM. Hence BCM (Boundary conduction mode), which is boundary between CCM and DCM i.e. when the magnetizing inductance current hits zero, the primary switch turns ON again, is the best mode to operate Flyback converter. Though BCM has sophisticated control strategy but is less complicated than control in CCM. There can be also done paralleling between two Flyback converters, which is known as interleaved structure can reduce the current spikes and stresses on switches in DCM. By operating secondary switch we can get power flow from grid to battery. Here in this thesis we have extended inversion operation to three phase. Similar to conventional grid connected inverter control for grid synchronisation and active, reactive power control we can apply similar principles on three phase single stage inverter. In future it is the aim is to operate Single-stage inverter in high power application.

## **References:**

1. *A GENERAL UNIFIED APPROACH TO MODELLING SWITCHING-CONVERTER POWER STAGES*, R. D. Middlebrook and Slobodan Cuk, California Institute of Technology Pasadena, California.
2. *A GENERAL UNIFIED APPROACH TO MODELLING SWITCHING DC-TO-DC CONVERTERS IN DISCONTINUOUS CONDUCTION MODE* SLOBODAN CUK and R. D. MIDDLEBROOK California Institute of Technology Pasadena, California.
3. *Use of Leading-Edge Modulation to Transform Boost and Flyback Converters into Minimum-Phase-Zero Systems*, Dan M. Sable, Bo H. Cho, Member, IEEE, and Ray B. Ridley
4. *Control of a Bidirectional Z-Source Inverter for Hybrid Electric Vehicles in Motoring, Regenerative Braking and Grid Interface Operations*. Omar Ellabban, Joeri Van Mierlo and Philippe Lataire.
5. *A Comparison between the Buck, Boost and Buck-Boost inverters* J. Almazbl, N. Vhunquez, C. Hernbdez, J. Alvarez, J. Arau
6. *Fundamentals of Power Electronics, SECOND EDITION*, University of Colorado Boulder, Colorado, Robert W. Erickson Dragan Maksimovic
7. *A Boost DC-AC Converter: Analysis, Design, and Experimentation*, Ram'on O. C'aceres, Member, IEEE, and Ivo Barbi, Senior Member, IEEE
8. *A novel single-stage inverter for the AC-module with reduced low-frequency ripple penetration*
9. *A Three-phase Soft-Switched High-Power-Density dc/dc Converter for High-Power Applications* Rik W. A. A. De Doncker, Member, IEEE, Deepakraj M. Divan, Member, IEEE, and Mustansir H. Kheraluwala, Student Member, IEEE
10. *Bidirectional DC-DC Converters for Energy Storage Systems*, Hamid R. Karshenas<sup>1,2</sup>, Hamid Daneshpajoo<sup>2</sup>, Alireza Safaee<sup>2</sup>, Praveen Jain<sup>2</sup> and Alireza Bakhshai<sup>2</sup> <sup>1</sup>Department of Elec. & Computer Eng., Queen's University, Kingston, <sup>2</sup>Isfahan University of Tech., Isfahan, <sup>1</sup>Canada <sup>2</sup>Iran
11. *Power transfer analysis in a single phase dual active bridge*, R. BARLIK, M. NOWAK, and P. GRZEJSZCZAK\_ Institute of Control and Industrial Electronics, Warsaw University of Technology, 75 Koszykowa St., 00-662 Warszawa, Poland
12. *Hybrid Modulation for Dual-Active-Bridge Bidirectional Converter With Extended Power Range for Ultracapacitor Application*, Haihua Zhou, Student Member, IEEE, and Ashwin M. Khambadkone, Senior Member, IEEE
13. *High-efficiency Bidirectional DAB Inverter using a Novel Hybrid Modulation for Stand-alone Power Generating System with Low Input Voltage*, Yong-Won Cho, Woo-Jun Cha, Jung-Min Kwon, Member, IEEE, and Bong-Hwan Kwon, Member, IEEE
14. *High Efficiency Bidirectional Grid-Tied Converter using Single Power Conversion with High Quality Grid Current*, Yeong-Seung Jeong, Sung-Ho Lee, Seo-Gwang Jeong, Jung-Min Kwon, Member, IEEE, and Bong-Hwan Kwon, Member, IEEE
15. *Grid-Connected Boost-Half-Bridge Photovoltaic Microinverter System Using Repetitive Current Control and Maximum Power Point Tracking* Shuai Jiang, Student Member, IEEE, Dong Cao, Student Member, IEEE, Yuan Li, Member, IEEE, and Fang Zheng Peng, Fellow, IEEE
16. *Flyback-Type Single-Phase Utility Interactive Inverter With Power Pulsation Decoupling on the DC Input for an AC Photovoltaic Module System* Toshihisa Shimizu, Senior Member, IEEE, Keiji Wada, Member, IEEE, and Naoki Nakamura

17. *Flyback Inverter Controlled by Sensorless Current MPPT for Photovoltaic Power System*  
Nobuyuki Kasa, Member, IEEE, Takahiko Iida, and Liang Chen
18. *A Simple Flyback Microinverter for Solar Energy Systems with Variable Frequency Controlled ZVS*  
Aniruddha Mukherjee Western University, Canada Department of Electrical Engineering London, ON, Canada N6A 5B9 [amukher7@uwo.ca](mailto:amukher7@uwo.ca) Majid Pahlevaninezhad Queen's University Department of Electrical Engineering Kingston, ON, Canada K7L 3N6 [7mp@queensu.ca](mailto:7mp@queensu.ca) Gerry Moschopoulos Western University, Canada Department of Electrical Engineering London, ON, Canada N6A 5B9 [gmoschop@uwo.ca](mailto:gmoschop@uwo.ca)
19. *Isolated Bidirectional Grid-Tied Three-Phase AC-DC Power Conversion using Series Resonant Converter Modules and a Three-Phase Unfolder*  
W. Warren Chen, Member, IEEE, Regan Zane, Senior Member, IEEE, and Luca Corradini, Senior Member, IEEE
20. *Superior decoupled control of active and reactive power for three-phase voltage source converters*  
Hesam RAHBARIMAGHAM, Erfan MAALI AMIRI, Behrooz VAHIDI\_, Gevorg BABAMALEK GHAREHPETIAN, Mehrdad ABEDI  
Department of Electrical Engineering, Amirkabir University of Technology, Tehran, Iran
21. *Control of Power Converters in AC Microgrids*  
Joan Rocabert, Member, IEEE, Alvaro Luna, Member, IEEE, Frede Blaabjerg, Fellow, IEEE, and Pedro Rodríguez, Senior Member, IEEE
22. *An Interleaved High-Power Flyback Inverter for Photovoltaic Applications*  
Bunyamin Tamyurek, Member, IEEE, and Bilgehan Kirimer
23. *Power Electronics: Converters, Applications, and Design* by Ned Mohan, Tore M. Undeland, William P. Robbins
24. *Power Electronics: Circuits, and Applications* by Muhammad H. Rashid, third edition